COMITATO NAZIONALE PER L'ENERGIA NUCLEARE
Laboratori Nazionali di Frascati

Proceedings of the Working Group on the Study of Photonuclear Reactions with Monochromatic and Polarized Gamma Rays.

Frascati, June 27 - July 5, 1973

Servizio Documentazione
dei Laboratori Nazionali di Frascati del CNEN
Casella Postale 70 - Frascati (Roma)

Laboratori Nazionali di Frascati del CNEN
Servizio Documentazione

LNF-73/62
27 Novembre 1973

Proceedings of the Working Group on the Study of Photonuclear Reactions with Monochromatic and Polarized Gamma Rays.

Frascati, June 27 - July 5, 1973

H. ARENHÖVEL - Institut fuer Kernphysik der Universitaet, Mainz (Germany)
S. COSTA - Istituto di Fisica dell'Università, and INFN Sezione di Torino
E. HAYWARD - National Bureau of Standards, Washington, D.C. (USA)
A. MARINO - CNEN, Laboratori Nazionali di Frascati
A. PASCOLINI - Istituto di Fisica dell'Università, and INFN Sezione di Padova
C. SCHAERF - CNEN, Laboratori Nazionali di Frascati
W. WEISE - Institut fuer Theoretische Physik der Universitaet, Erlangen-Nürnberg (Germany)

PREFACE. -

Presenting the proceedings of the Frascati working group on the study of photonuclear reactions with monochromatic and polarized gamma rays I wish to thank the Laboratori Nazionali di Frascati and in particular their director Prof. I.F. Quercia whose hospitality and collaboration made this venture possible.

The working group was organized by the Laboratori Nazionali di Frascati to study the most immediate applications to the investigation of photonuclear reactions of monochromatic and polarized gamma ray beams. It was originated by a proposal to produce a medium energy ($\lesssim$150 MeV) photon beam by the Compton scattering of laser light against the high energy (E = 1500 MeV) electrons circulating in the storage ring Adone. At this very high laboratory energy the backward scattered photons retain the original polarization, and the final energy is defined by the angle of scattering. There is no intrinsic competing process which produces photons of different energy.

The working group has met in Frascati only for one week. This very limited time deeply influenced the number of all the interesting possibilities which could be examined. The working group had to confine itself only to the problems already known to its members and available in the published literature. Moreover the attention devoted to the different topics does not reflect their relative importance but the amount of information at hand. The working week was followed by a short symposium in which the results of the working group were presented and exposed to the criticism of a large group of physicists interested in these problems. A consensus emerged that the proposed facility will open new interesting possibilities to the experimental investigation of photonuclear reactions and will permit the extension of fundamental measurements to energy regions now unexplorable. For its characteristics the proposed beam is an ideal match to the monochromatic photon beam obtainable by positron annihilation in flight.

As it is evident from the final remarks, a beam with an intensity around 10^7 photons per second will produce in a reasonable time data with good statistical accuracy for all the experiments here considered.

Carlo Schaerf

I.- EXPERIMENTAL CONSIDERATIONS.-

In this chapter we will discuss the possibility to obtain a beam of monochromatic and polarized gamma rays by the Compton scattering of laser light on the high energy electrons circulating in a storage ring.

The high power now available from continuous ion lasers and the large number of electrons circulating in a storage ring make feasible a photon beam of sufficient intensity to perform most advanced experiments in the field of photonuclear reactions.

1.- Compton scattering on high energy electrons.-

Kinematics.-

In the Compton scattering on moving electrons the energy of the scattered photon is given[1] by the following formula:

$$k = \omega \frac{1 - \beta \cos\theta_1}{1 - \beta \cos\theta + \frac{\omega}{E}(1 - \cos\theta_2)} \tag{1}$$

Our notation is the following:

ω energy of the incident photon,
k energy of the scattered photon,
E, p energy and momentum of the incident electron,
β velocity of the incident electron in units of c,
m electron mass,
θ_1 angle between the directions of the incident electron and the incident photon,
θ_2 angle between the directions of the incident and scattered photon,
θ angle between the direction of the incident electron and the scattered photon,
$\gamma = E/m$
$z = 4(E\omega/m^2)$.

The maximum energy k_{max} of the scattered photon is obtained for the following values of the parameters:

$$\theta_1 = \pi ; \qquad \theta_2 = \pi ; \qquad \theta = 0$$

and for very high energy electrons ($E \gg m$) is given by:

$$k_{max} = \frac{4\omega\gamma^2}{1+z} \tag{2}$$

In our case: E = 1500 MeV, ω = 2.54 eV, z = 0.0584 and k_{max} = 83 MeV.

For:

$$\theta_1 \approx \pi ; \qquad \theta_2 \approx \pi ; \qquad \theta < \frac{1}{\gamma}$$

the energy of the scattered photon is very sensitive to the value of θ and insensitive to θ_1 and θ_2.

We can write with good approximation:

$$k \simeq 4\omega\gamma^2 \left[1 + z + (\gamma\theta)^2\right]^{-1} \tag{3}$$

This formula gives the energy dispersion of the scattered photon beam as a function of the

scattering kinematics. The angle θ, between the direction of the incident electron and the scattered photon, can be defined not better than the angular dispersion of the primary electron beam. This dispersion is of the order of 10^{-4} rad.(2). Since $\Delta E/E$ is usually less than 10^{-3} and $\Delta\omega/\omega$ completely negligible, $\Delta\theta$ is the only relevant contribution to Δk.

Therefore we can use the following expressions:

$$\frac{\Delta k}{k_{max}} \simeq (\gamma\,\Delta\theta)^2 \simeq (\Delta\theta)^2\,\frac{k_{max}}{4\omega} \tag{4}$$

which in our case:

$$\Delta\theta = 10^{-4}; \qquad \gamma = 2950;$$

give:

$$\frac{\Delta k}{k_{max}} = 0.081, \qquad \text{and} \qquad \Delta k = 6.7\ \text{MeV}$$

Cross section.

The total cross section in our energy region is given with a good approximation by the classical Thompson formula:

$$\sigma_T = \frac{8}{3}\pi r_o^2 = 0.665\ \text{barn}$$

$r_o = 2.81777$ fermi, is the classical electron radius.

The differential cross section in the laboratory system is:

$$\frac{d\sigma}{d\Omega} = r_o^2\,\frac{2}{m^2 x_1^2}\left[4\left(\frac{1}{x_1}+\frac{1}{x_2}\right)^2 - 4\left(\frac{1}{x_1}+\frac{1}{x_2}\right) - \left(\frac{x_1}{x_2}+\frac{x_2}{x_1}\right)\right]\omega^2$$

where for $\theta_1 = \pi$ x_1 and x_2 are given by:

$$x_1 = 2\omega(E+p)/m^2 = z\,\frac{(1+\beta)}{2}; \qquad x_2 = 2k(E-p\cos\theta)/m^2$$

The differential photon spectrum and the differential photon energy spectrum are given in Fig. 1 for our values of the parameters ($E = 1500$ MeV, $\omega = 2.54$ eV). In the abscissa of the same figure are indicated also the angles at which photons of a given energy are scattered. Therefore, from this figure we can visualize the energy spectrum of the secondary photon beam as a function of its angular acceptance. In our case the resulting photon spectrum is indicated by the solid line of Fig. 2 where the angular resolution of the primary electron beam is of the order of 10^{-4} radiants and therefore a similar collimation of the final photons can be assumed. This suggests an energy resolution of 6 MeV, a result in good agreement with the approximate expression 4.

Photon Polarization. -

For very relativistic electrons their elicity is a good quantum number. Therefore, the electron spin-flip amplitude is negligible and the backward scattered photons retain their original polarization. If we use a laser with Brewster windows which produce plane polarized light, the high energy photons produced by Compton scattering will have similar polarization. This polarization has been calculated (3) as a function of the scattering angle and the corresponding final photon energy. The numerical results, for our values of the kinematical variables, are indicated in Fig. 3. For a scattering angle of 10^{-4} rad this polarization is larger than 0.98.

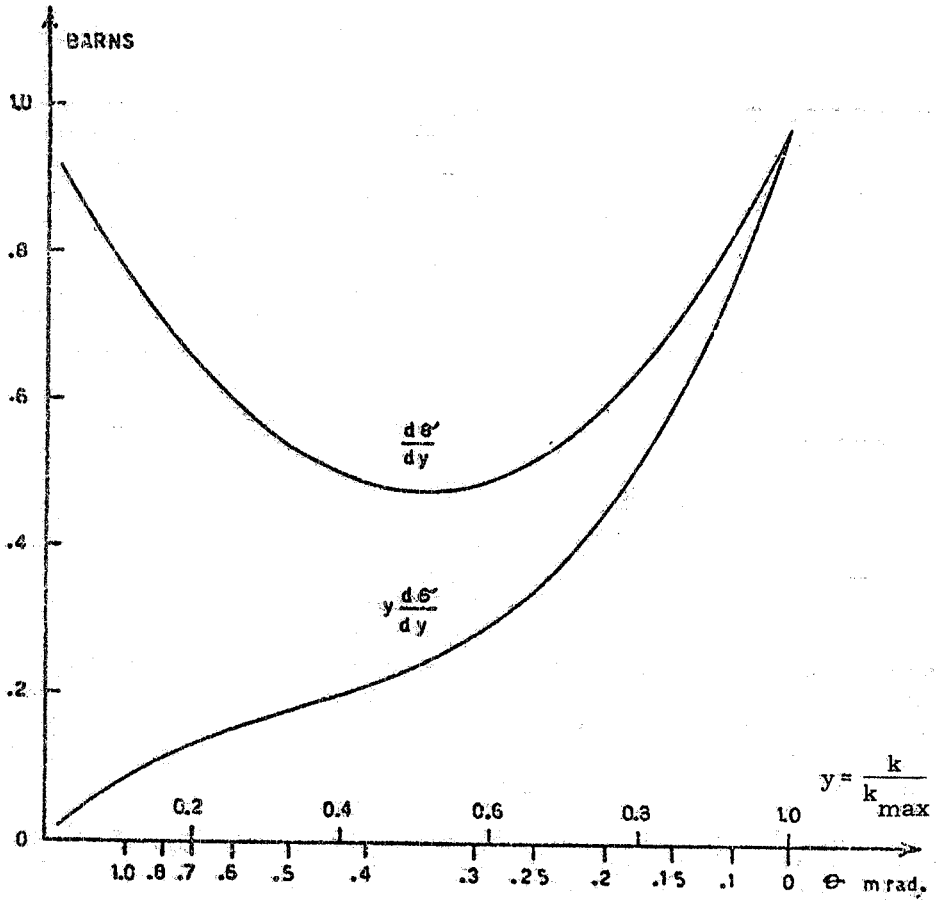
BARNS
1.0
.8
.6
.4
.2
0
$\frac{d\sigma'}{dy}$
$y\frac{d\sigma'}{dy}$
$y = \frac{k}{k_{max}}$
0.2
0.4
0.6
0.8
1.0
1.0 .8 .7 .6 .5 .4 .3 .25 .2 .15 .1 0 Θ m rad.

FIG. 1

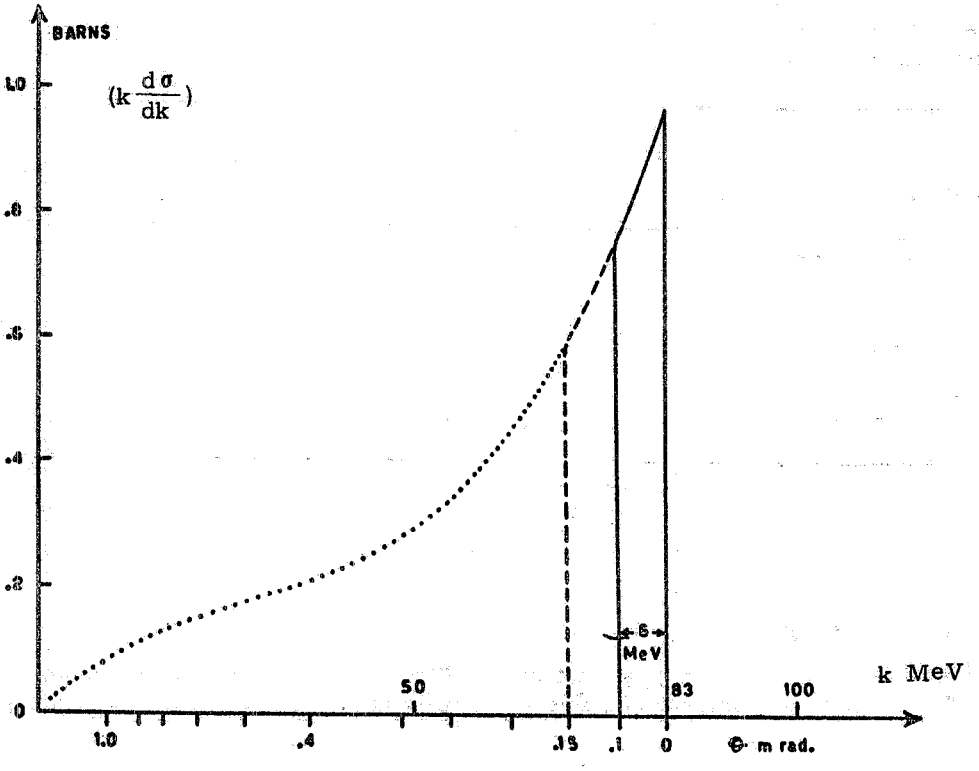
BARNS
$(k\frac{d\sigma}{dk})$
1.0
.8
.6
.4
.2
0
δ MeV
50
83
100
k MeV
1.0
.4
.15
.1
0
Θ m rad.

FIG. 2

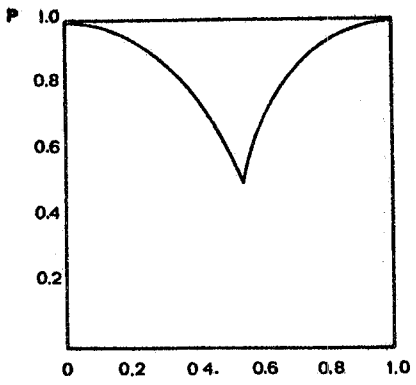

$$y = \frac{k}{k_{max}}$$

FIG. 3

2.- Laser beam interaction region.-

In order to obtain a beam of high energy and high intensity photons we must start with an incident beam of high frequency and high intensity. A good compromise is a Ion Argon laser which produces a beam of blue-green light of 2.54 eV (488 nm) and a power of some watts. The internal beam of a laser resonator modified as to superimpose itself to a straight section of the storage ring has been used in order to increase the photon density in the interaction region.

A commercial Argon laser with an output power of 4 W normally uses an output mirror with a transmission of 5%. This implies that the internal power of the laser is 80 W. By using an output window totally reflecting, (i.e. with a reflectivity larger than 99.7%) the cavity loss is decreased by an order of magnitude and a similar factor in the internal power should be gained. However, to superimpose the cavity to the straight section of the storage ring, the cavity length must be increased almost by an order of magnitude (more than 12 meters). This will obviously produce a decrease in the internal power. Taking into account all the losses introduced by the other components of the full cavity, we can reasonably assume to have a useful power of 300 W.

An other parameter is the cross section of the beam represented by the distance, ϱ, from the beam axis where its intensity is reduced by a factor of e. We are interested in having the smallest possible value of ϱ in the interaction region. To obtain this, we are now in the preliminary stage of realizing a cavity as the one indicated in Fig. 4. In this figure M_1 is a flat surface totally reflecting mirror, M_2 a similar one with a radius of curvature of 10 m and L is a lens with a focal length of 2.65 m. The calculated values of the radius are represented at some points of particular interest. The mean radius in the interaction region is 1 mm.

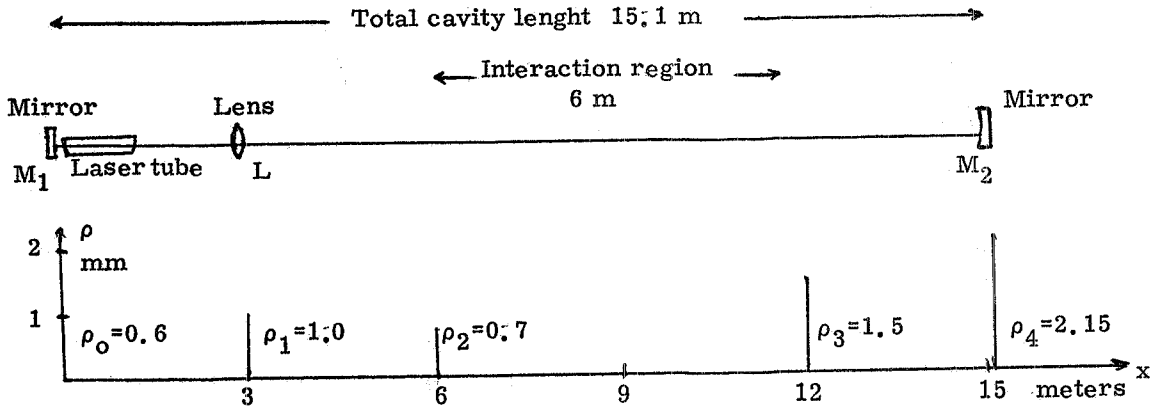

FIG. 4

3.- Photon yield.-

The yield of high energy photons is determined by the number of high energy electrons, the number of incident photons and the geometry of the interaction region. It is given by:

$$\frac{\dot{dn}}{dk} = \frac{d\sigma}{dk} c \int_V n_e n_\gamma \, dV$$

where:

$\frac{\dot{dn}}{dk}$ indicates the photon yield per MeV and per second;
c velocity of light
n_e electron density per unit volume
n_γ photon density per unit volume.

The integral is extended over the entire volume of the interaction region.

To first approximation we will assume that the electron and photon densities remain constant in the length of the interaction region and are rapidly varying functions of the transversal variables x and y. These latter variations are assumed to have two dimensional gaussian distributions of the form:

$$n_e = n_{oe} \exp\left(-\frac{x^2}{\zeta^2} - \frac{y^2}{\eta^2}\right), \qquad n_\gamma = n_{o\gamma} \exp\left(-\frac{x^2+y^2}{\varrho^2}\right)$$

ζ, η and ϱ are the values of x, y and $r = \sqrt{x^2+y^2}$ where the densities are reduced by a factor of e with respect to the maximum (at x=y=0). If the densities are not constant in the length of the interaction region some mean values must be assumed. From this we obtain:

$$\frac{\dot{dn}}{dk} = \frac{d\sigma}{dk} \frac{N_e P}{2\pi^2 \omega e} \frac{1}{R} (\zeta^2 + \varrho^2)^{-1/2} (\eta^2 + \varrho^2)^{-1/2} \tag{4}$$

where:

N_e is the number of electrons circulating in the storage ring;
P is the power of the laser beam in watt;
l is the length of the interaction region in meters;
R is the mean geometrical radius of the electron's orbit measured in meters;
e is the electron charge: 1.6×10^{-19} Coulomb.

Formula 4 must be corrected for the effect of beam instability in the storage ring. This can be accounted introducing a new parameter χ which represents the short term root mean square displacement of the beam from the equilibrium orbit. With this correction our final formula is:

$$\frac{\dot{dn}}{dk} = \left(\frac{d\sigma}{dk} \frac{1}{\sigma_T}\right) N_e P \frac{\sigma_T}{2\pi^2 \omega e} \frac{1}{R} (\varrho^2 + \chi^2 + \zeta^2)^{-1/2} (\varrho^2 + \chi^2 + \eta^2)^{-1/2} \tag{5}$$

where $\sigma_T = 0.665$ barn is the Thompson total cross section. For the storage ring Adone we can assume:

$N_e = 2 \times 10^{11}$, $R = 16.7$ m, $l = 6.0$ m, $\zeta = 1.5$ mm, $\eta = 0.5$ mm, $\chi = 0.5$ mm

And for our calculated laser cavity:

$$P = 300 \text{ W}, \quad \omega = 2.54 \text{ eV}, \quad \varrho = 1 \text{ mm}.$$

Which gives:

$$\frac{\dot{dn}}{dk} = 7.8 \times 10^7 \left(\frac{d\sigma}{dk} \frac{1}{\sigma_T}\right)$$

The number of photons per unit time in a given energy interval Δk is given by:

$$\dot{n} = \left(\frac{d\sigma}{dy}\, y\right) \frac{1}{\sigma_T} \frac{\Delta k}{k} 7.8 \times 10^7$$

From Fig. 1 and for an energy interval of 8%:

$$\frac{d\sigma}{dy}\, y = 0.84 \text{ barn}, \qquad \frac{\Delta k}{k} = 0.08, \qquad \dot{n} = 8 \times 10^{6} \text{ fotoni sec}^{-1}$$

4.- Background photons.-

The bremsstrahlung of the circulating electrons against the nuclei of the residual gas in the storage ring vacuum chamber is the only appreciable source of background photons. The total power radiated in this way is given by:

$$W_B = t \frac{N_e c}{2\pi R} E a$$

where many symbols have been previously defined and:

a is the fraction of gamma rays accepted by our solid angle. In our case we can assume: $\Delta\Omega \approx \pi\, \theta^2 \approx 3 \times 10^{-8}$ ster and from Fig. 4 of ref. (4) we obtain:

$$a = \frac{8.6}{108.6} = 0.08$$

t is the thickness of gas traversed by the electrons in a straight section measured in units of its radiation length:

$$t = \frac{l\, p}{X_o\, 765}$$

$l = 6$ m, is the length of the straight section,
$p = 10^{-9}$ torr is the pressure in the vacuum chamber,
$X_o = 3029$ m is the radiation length of the residual gas assumed to be air,

$$t = 2.6 \times 10^{-14}$$

The final result is:

$$W_B = 1.8 \times 10^{6} \text{ MeV/sec}$$

at an electron energy of 1500 MeV.

This number must be compared with the total power in the beam of Compton scattered photons:

$$W_C = \dot{n}\, k = 8 \times 10^{6} \times 83 = 6.6 \times 10^{8} \text{ MeV/sec}$$

Therefore the ratio of the background power to the power of the signal is given by:

$$r_w = \frac{W_B}{W_C} = 0.27 \times 10^{-2}$$

We can also calculate the number of background photons present in an energy interval equal to that of the signal. This is given by:

$$\dot{n}_B = \frac{\Delta k}{k} \frac{W_B}{E}$$

for an energy interval of 8% the result is:

$$\dot{n}_B = 96 \text{ sec}^{-1}$$

The ratio of the background photons to the useful ones in the same energy interval is given by:

$$r_n = \frac{\dot{n}_B}{\dot{n}_C} = 1.2 \times 10^{-5}$$

5. - Experimental apparatus. -

The experimental apparatus which we consider now is indicated in Fig. 5. The resonating laser cavity (15.1 m long) contains one of the straight section of the storage ring Adone. The high energy photons produced by Compton scattering pass through one mirror of the laser resonator and travel in a vacuum pipe to the collimator. The angle of collimation being of the order of 10^{-4} rad, and the source size of the order of 1 mm, the hole of the collimator must be several millimeters in diameter and therefore the collimator must be at least 30 meters from the interaction region. We are considering placing the collimator at a distance between 30 and 60 meters from the interaction region. A longer distance would increase too much the size of the gamma ray beam in the experimental area. This experimental area is situated after the collimator at a distance of a few meters to allow for appropriate shielding (not a serious problem in our case) and for comfortable set up of the experiments.

More than one experiment can be installed on the same beam line. Provided that the preceeding ones do not alter appreciably the photon spectrum. they can operate simultaneously. A total absorption counter which counts individual photons with high efficiency can provide an accurate monitor for all the experiments.

Some of the main features of the proposed photon beam are summarized in Table I where they are compared with other photon facilities. The distinctive characteristics of our beam are the absence of any appreciable background and the total polarization.

II. - PHOTON SCATTERING. -

Introduction. -

There are four coherent scattering amplitudes for the scattering of photons by nuclei, that can produce interference in such a way that they are difficult to determine separately[5].

They are:

1) the energy independent Thomson scattering amplitude $D = -Z^2e^2/AMc^2$,
2) Rayleigh scattering from bound electrons which is peaked strongly forward and is only important at low energies,
3) nuclear scattering from bound levels and the continuum, in particular the Giant Dipole Resonance and the E2 Giant Resonance (this latter scattering has not yet been observed),
4) Delbrück scattering which is associate with pair production and is therefore very large though concentrated in the forward direction.

A general discussion of these processes may be found in reff. (6) and (7): here we will consider the aspects more relevant at intermediate energies and the possibilities given by polarized monochromatic gamma rays sources.

1. - Delbrück scattering. -

Delbruck scattering is the scattering of light by the vacuum polarization cloud created in the vicinity of a charged particle by its Coulomb field. The basic process is the virtual creation and subsequent annihilation of an electron-positron pair (see Fig. 6). It is a genuine quantum electrodynamic process and is, therefore, of considerable interest.

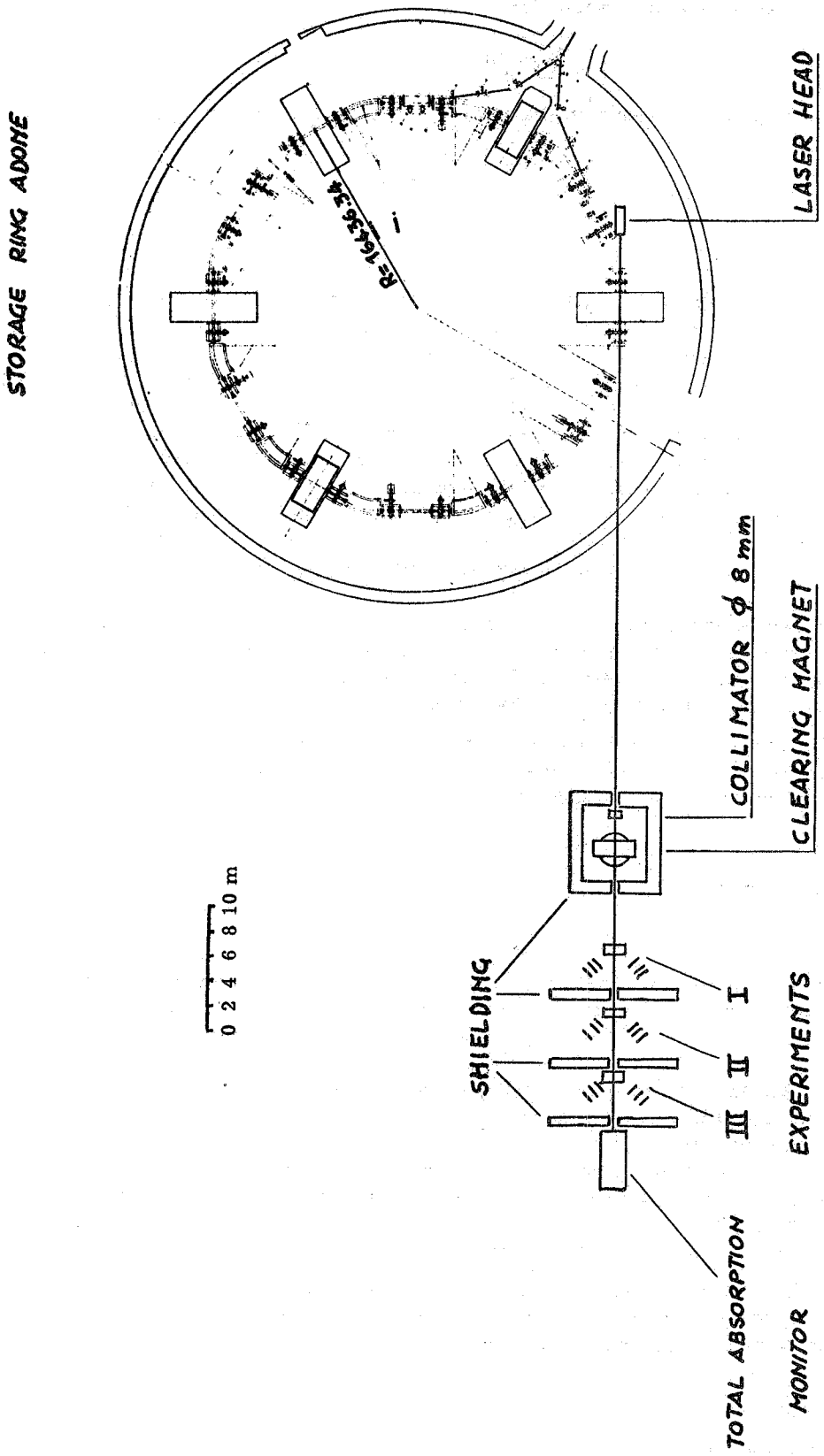
STORAGE RING ADONE
R=1636.4
LASER HEAD
COLLIMATOR ϕ 8 mm
CLEARING MAGNET
SHIELDING
I
II
III
EXPERIMENTS
TOTAL ABSORPTION
MONITOR
0 2 4 6 8 10 m

FIG. 5

TABLE I

1	2	3	4	5	6	7	8	9	10	11	12	13	14	15	16
Technique used	Accelerator considered	Incident particle	Target material and thickness gr/cm^2	Incident energy MeV	Angular resolution of primary beam and experimental apparatus mrad	Number of incident particles sec^{-1}	Photon energy MeV	Line width of monocromatic photons FWHM MeV	Number of photon produced sec^{-1}	$r_n = N_B/N_\gamma$	$r_W = W_B/W_\gamma$	Polarisation	Macroscopic duty cicle	Machine operating freq. MHz	Notes
Coherent bremsstrahlung	FRASCATI LINAC	e^-	Be Xstal 9.25×10^{-3}	375	0.41	10^{13}	75	10	2.3×10^8	0.12	1.6	0	<1‰	irrelevant	$\alpha=0^\circ$
					0.41	10^{13}	75	9	2.3×10^8	0.18	2.8	0.56			$\alpha=90^\circ$
					0.41	10^{13}	75	9	2.3×10^8	0.26	4.2	0.74			$\alpha=74.56^\circ$
					0.41	10^{13}	75	8	2.3×10^8	0.17	4.2	0.80			$\alpha=74.56^\circ$
Coherent bremsstrahlung	FRASCATI ELECTRO SINCHROTRON	e^-	C Xstal 7×10^{-3} (0.02mm)	1000	0.1	10^{11}	75	8	7.5×10^6	0.01	3.5	0.80	5%	~40	$\alpha=13.26^\circ$
Laser Compton scattering	FRASCATI STORAGE RING ADONE	e^-	Argon Laser 6 Watt Interaction region 6 m	1500	0.1	10^{18}	83	7	$\sim10^7$	$<10^{-4}$	$<10^{-2}$	0.98	1	50	
Laser Compton scattering	FRASCATI STORAGE RING ADONE	e^-	Argon Laser 6 Watt Interaction region 6 m	750	0.1	10^{18}	21	0.5	$\sim10^7$	$<10^{-4}$	$<10^{-2}$	0.98	1	50	

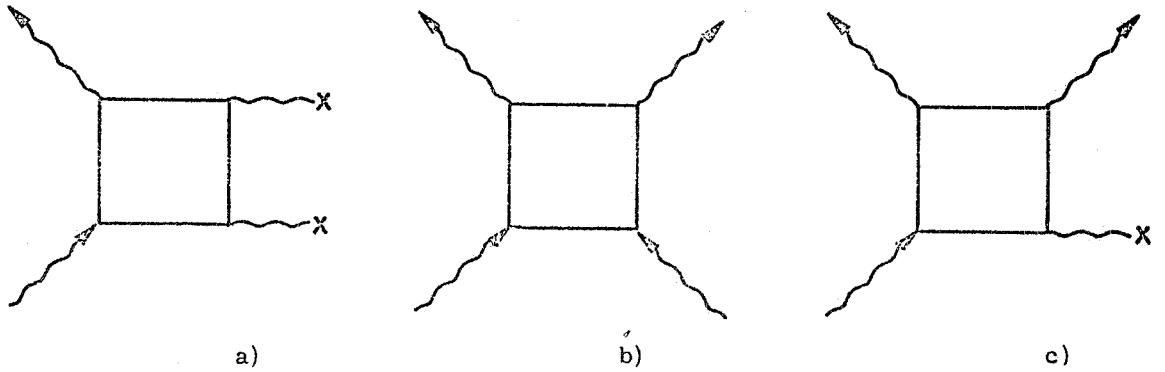

FIG. 6

Its absorbtive part describes the pair production in a Coulomb field. The knowledge of the Delbrück scattering amplitude is furthermore very important for the determination of the nuclear photon scattering amplitude in the forward direction ($\theta < 90^{o}$). At high energies the Delbrück scattering cross section is the dominant one at forward angles.

In recent years two unambiguous measurements[8, 9] of this phenomenon have been made at low energy, by making use of neutron capture γ-rays and very high resolution Ge(Li) detectors. Their results compare favourably with the calculations of Ehlotzky and Sheppey[10], who give the only Delbrück amplitudes at low energy at other than very small angles. However, uncertainties in the knowledge of the Rayleigh amplitudes hamper this comparison. At high energies the comparison with QED predictions is easier since Rayleigh scattering can be neglected. A recent experiment[11], carried out at very high energies (between 1 and 7.3 GeV) using a well collimated bremsstrahlung beam from the DESY electron synchrotron, gives results in good agreement with the calculations of Cheng and Wu[12], valid for high energies and not too small momentum transfers, if Coulomb corrections are included. Figg. 7a and b give the differential cross sections calculated by Cheng e Wu, and

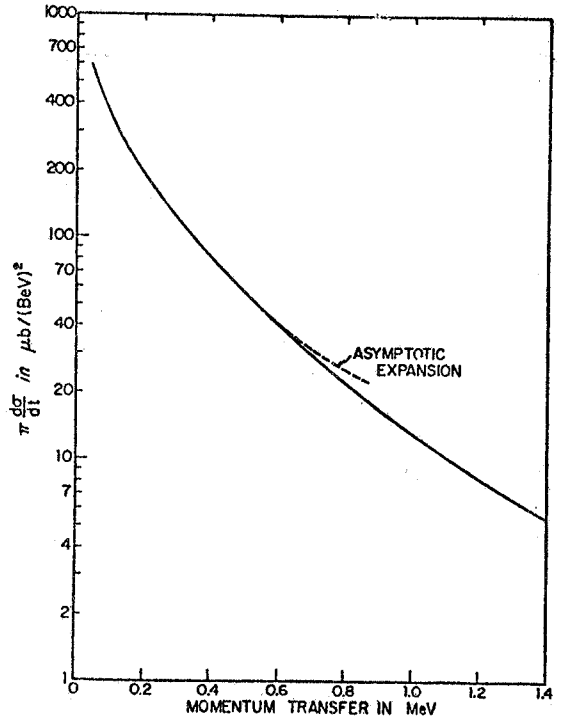

FIG. 7a - Differential cross sections at high energies. (To get $d\sigma/d\Omega$ in μb/sr for a nucleus of charge Ze, multiply, by $Z^4 \omega^2$, where ω is the energy of the photon in BeV).

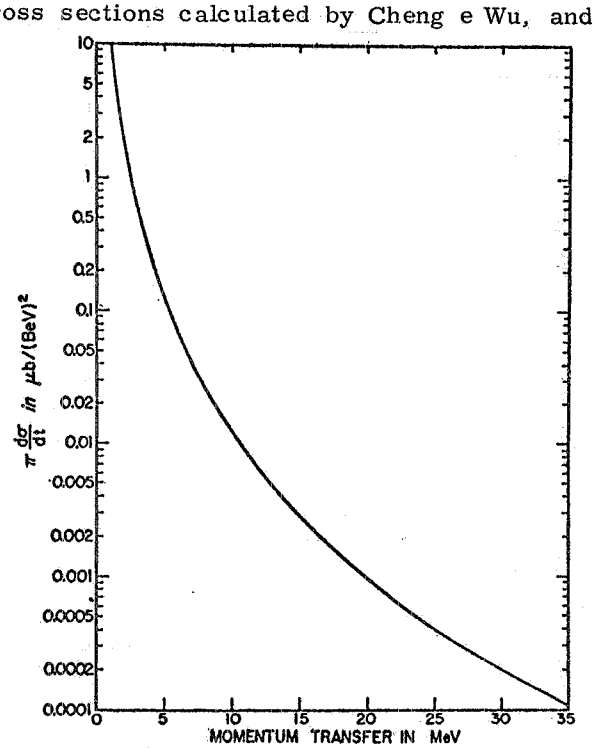

FIG. 7b - Differential cross sections at high energies (continued).

Fig. 8 their results for polarized photons; these calculations are valid for energies of about 80 MeV, where only an old experiment[13] has yet been done, with a poor energy resolution.

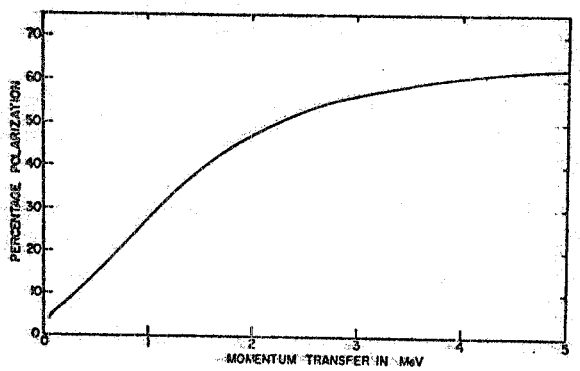

FIG. 8 - Polarization of the scattered photon at high energies when the incident photon is unpolarized.

An experiment using monochromatic polarized photons in this energy range would be very interesting. At angles of say 10^{o} the cross section should be very large compared to any nuclear scattering cross section and the more intense Compton scattered photons are reduced in energy sufficiently to be separated from the elastically scattered photons by NaI(Tl) spectroscopy. The cross section varies as Z^4 so it is a good idea to begin considering U as a target. Using Cheng and Wu calculations, at 90 MeV we can estimate the Delbrück scattering cross sections parallel and perpendicular to the polarization vector at 10^{o}:

$$(d\sigma/d\Omega)^{\shortparallel}(U, 10^{o}) = 4.54 \text{ mb/ster}, \qquad (d\sigma/d\Omega)^{\perp}(U, 10^{o}) = 0.96 \text{ mb/ster}.$$

These cross sections are larger at higher energies and a steep function of angle.

Finally we would like to remark that at a particular energy below the GDR the nuclear scattering amplitude vanishes because of destructive interference between nuclear Thomson and nuclear resonance scattering. For that energy the scattering amplitude would be pure Delbrück plus Rayleigh.

2.- The nuclear scattering of plane polarized photons by the E1 Giant Resonance.-

The combination of nuclear electric dipole scattering and nuclear Thomson scattering has been studied at large angles for many years[14]. It has an angular distribution varying as $1+\cos^2\theta$ for unpolarized incident photons and $I = 0$ nuclei. Incoherent nuclear scattering can also take place if the nucleus has some intrinsic asymmetry[15] such as a spin different from zero or a deformation be it permanent or transitory. This scattering has an almost isotropic angular distribution, $13+\cos^2\theta$.

The motivation of doing photon scattering in the E1 giant resonance is to investigate the structure of the GDR, in particular, to study the question whether this structure can be understood as a coupling of the low lying collective states to the GDR as is described, e.g., in the Dynamic Collective Model[16].

This model is an extension of the hydrodynamic model which takes into account the coupling between the GDR and the quadrupole oscillations of the nuclear surface. As a result of this coupling the GDR can deexcite by populating the low-lying vibrational states that can be reached in electric dipole transitions. This inelastic scattering is in addition to the coherent elastic scattering, that is related to the absorption cross section by the optical theorem and dispersion relations, as well as the scattering which populates the ground-state rotation bands of ellipsoidal nuclei. The inelastic scattering that results from the nuclear surface oscillations has the same angular momentum properties as that which populates the rotational band since it, too, results from the transfer of two units of angular momentum to the nucleus in the two-step scattering process. The Dynamic Collective Model predicts the relative intensities of all of these different components in the scattering cross section; it is, therefore, important to make measurements in order to check the calculations and help to improve the model.

For the deformed nuclei much better measurements are required to determine whether there are indeed transitions to the γ-vibrational band and thus whether there is even a need for the dynamic collective model. Because the inelastic scattering populating the 2^+ γ-vibrational state vanishes in the simple rotator model, while the Dinamic Collective Model predicts considerable strengths in that case.

For the spherical nuclei we need good measurements to ascertain the influence of anharmonicities in the surface vibrations. For transition nuclei these measurements can help in understanding their collective character.

In spite of the fact that the hydrodynamic model is not applicable to light nuclei, we know that the GDR is coupled to the low-lying states. The photon scattering experiments using plane polarized photons can certainly throw some light on the magnitude and energy dependence of this interaction.

In electric dipole approximation the photon scattering cross section is[17]

$$(1) \qquad d\sigma/d\Omega = \sum_{\nu=0}^{2} |A_\nu|^2/(2\nu+1)\, g_\nu(\theta)$$

where ν is the angular momentum transferred to the nucleus and can be 0, 1, or 2. We neglect $\nu = 1$ because its amplitude is very small. The A_ν are the scattering amplitudes and the $g_\nu(\theta)$ contain the angular distributions and polarizations. For plane polarized incident radiation with the polarization vector perpendicular to the plane of scattering and parallel, respectively, explicit expressions and values of functions $g_\nu(\theta) = g_\nu(11\,\theta)$ are given in Tabella IIa. With these expressions we have

$$(2) \qquad \begin{aligned} d\sigma^{\perp}/d &= 1/3\,|A_0|^2 + 7|A_2|^2/30\,, \\ d\sigma''/d\Omega &= 1/3|A_0|^2\cos^2\theta + 1/5|A_2|^2(1+1/6\cos^2\theta) \end{aligned}$$

and for $\theta = \pi/2$

$$d\sigma''/d\Omega = 1/5|A_2|^2\,.$$

This says, of course, that the nucleus has no coherent ($\nu = 0$) scattering along the polarization vector, so that a measurement of photon scattering in this direction is a measure of the incoherent ($\nu = 2$) scattering, that in a spherical nucleus populates the low-lying vibrational levels.

In heavy nuclei these vibrational levels are so close to the ground state that it is not practical to separate the coherent and the incoherent components in the scattering by γ-ray spectroscopy. The trick is to use a poor resolution NaI(Tl) spectrometer which automatically sums both contributions. A measurement of $d\sigma^{\perp}/d\Omega$ and $d\sigma''/d\Omega$ then allows the determination of two scattering amplitudes. It is straightforward to make the two measurements simultaneously using two spectrometers.

The above discussions refer only to electric dipole transitions. Were there, for example, M1 strength buried in the giant resonance, it would also show up as scattering along the polarization vector. For energies above the giant resonance there surely is E2 strength and at some energy it will mask the incoherent E1 scattering.

A recent experiment[18] has demonstrated the possibility of studying the E1 giant resonance using plane polarized incident photons. In this experiment plane polarized photons produced in the resonance fluorescence of the 15.1 MeV, 1^+ state in ^{12}C were used to excite the GDR of heavy nuclei. The results of this experiment are very crude indeed because of large statistical errors, and, since only this 15.1 MeV excitation energy was available, it is limited to nuclei at most as heavy as Cadmium. The availability of an intense beam of plane polarized, monochromatic photons having energies variable throughout the GDR would allow this important experiment to be performed with much greater accuracy and permit its extension to a wide range of energies and nuclei.

TABLE IIa

$g_o^{\perp}(11\,\theta) = 1/3$	$g_o^{\perp}(11\,\pi/2) = 1/3$
$g_o''(11\,\theta) = 1/3\cos^2\theta$;	$g_o''(11\,\pi/2) = 0$
$g_1^{\perp}(11\,\theta) = 1/2$	$g_1^{\perp}(11\,\pi/2) = 1/2$
$g_1''(11\,\theta) = 1/2\,(2-\cos^2\theta)$	$g_1''(11\,\pi/2) = 1$
$g_2^{\perp}(11\,\theta) = 7/6$	$g_2^{\perp}(11\,\pi/2) = 7/6$
$g_2''(11\,\theta) = 1+1/6\cos^2\theta$	$g_2''(11\,\pi/2) = 1$
$g_o^{\perp}(22\,\theta) = \cos^2\theta/5$	$g_o^{\perp}(22\,\pi/2) = 0$
$g_o''(22\,\theta) = 1/5\,(1-4\cos^2\theta\,\sin^2\theta)$	$g_o''(22\,\pi/2) = 1/5$
$g_1^{\perp}(22\,\theta) = 4/9\,(2-\cos^2\theta)$	$g_1^{\perp}(22\,\pi/2) = 8/9$
$g_1''(22\,\theta) = 4/9\,(1+16\cos^2\theta\,\sin^2\theta)$	$g_1''(22\,\pi/2) = 4/9$
$g_2^{\perp}(22\,\theta) = 1/14\,(6+\cos^2\theta)$	$g_2^{\perp}(22\,\pi/2) = 3/7$
$g_2''(22\,\theta) = 1/14\,(7-16\cos^2\theta\,\sin^2\theta)$	$g_2''(22\,\pi/2) = 1/2$
$g_3^{\perp}(22\,\theta) = 1/5\,(3-\cos^4\theta+\sin^4\theta)$	$g_3^{\perp}(22\,\pi/2) = 4/5$
$g_3''(22\,\theta) = 1/5\,(3-\cos^4\theta-\sin^4\theta)$	$g_3''(22\,\pi/2) = 2/5$
$g_4^{\perp}(22\,\theta) = 2/35\,(10+4\cos^2\theta)$	$g_4^{\perp}(22\,\pi/2) = 4/7$
$g_4''(22\,\theta) = 2/35\,(14-\cos^2\theta+\cos^4\theta)$	$g_4''(22\,\pi/2) = 4/5$
$g_o^{\perp}(12\,\theta) = \left[\cos\theta(\sin^2\theta-\cos^2\theta)\right]/\sqrt{15}$	$g_o^{\perp}(12\,\pi/2) = 0$
$g_o''(12\,\theta) = -\cos\theta/\sqrt{15}$	$g_o''(12\,\pi/2) = 0$
$g_1^{\perp}(12\,\theta) = -\cos\theta(1+4\sin^2\theta)/2\sqrt{5}$	$g_1^{\perp}(12\,\pi/2) = 0$
$g_1''(12\,\theta) = -\cos\theta/2\sqrt{5}$	$g_1''(12\,\pi/2) = 0$
$g_2^{\perp}(12\,\theta) = -\cos\theta\,(1+4\cos^2\theta)/2\sqrt{21}$	$g_2^{\perp}(12\,\pi/2) = 0$
$g_2''(12\,\theta) = -5\cos\theta/2\sqrt{21}$	$g_2''(12\,\pi/2) = 0$

TABLE IIb

Some Special Functions and Coefficients

$P_o(\cos\theta) = 1$	$P_2^2(\cos\theta) = 3\sin^2\theta$	$f_2(11) = -1/2$
$P_1(\cos\theta) = \cos\theta$	$P_3^2(\cos\theta) = 15\sin^2\theta\cos\theta$	$f_2(12) = -1/6$
$P_2(\cos\theta) = 1/2\,(3\cos^2\theta-1)$	$P_4^2(\cos\theta) = 15/2\,(\sin^2\theta)(7\cos^2\theta-1)$	$f_2(22) = 1/2$
$P_3(\cos\theta) = 1/2\,(5\cos^3\theta-3\cos\theta)$		$f_3(12) = -1/6$
$P_4(\cos\theta) = 1/8\,(35\cos^4\theta-30\cos^2\theta+3)$		$f_3(22) = 0$
		$f_4(22) = -1/12$

3.- The nuclear scattering of plane polarized photons including Electric Dipole and Quadrupole Transitions.-

Now we ask whether there is any way we can learn anything about the E2 giant resonance by simply extending the above-mentioned scattering experiment into that energy re region. Arenhövel and Greiner[7] have given the angular distribution formulae for electric dipole and quadrupole radiations including polarization in the incoming and outgoing channels. Here we specialize to the case of 100% plane polarized incident radiation and no polarization analysis for the outgoing radiation: generalizing the notation of (5) and (6), we have:

$$(3) \qquad d\sigma^{''\perp}/d\Omega = \sum_{\nu, LL'} A_\nu(EL)^{*} A_\nu(EL') \, g_\nu^{''\perp}(LL'\theta)/(2\nu+1)$$

the angular distributions for incident radiation polarized perpendicular and parallel to the scattering plane being given, with their value for $\theta = \pi/2$ in Table IIb. The interference terms, of course, have no contributions at $\pi/2$. The E1 scattering along the polarization vector and the E2 scattering perpendicular to it are also zero for coherent scattering ($\nu = 0$). For values of $\nu \neq 0$, the $g_\nu^{''\perp}(LL' \pi/2)$ are almost of the same magnitude and produce an almost isotropic azimuthal angular distribution. For this reason it would not be instructive to measure the scattering cross section parallel and perpendicular to the polarization vector in an experiment where the detector integrates over the final states at an excitation energy where there are contributions from both E1 and E2 absorption.

On the other hand, if it is possible to separate only the coherent ($\nu = 0$) scattering from the other components in the scattering cross section, then one can make a definitive identification of the E1 and E2 amplitudes, since at $\theta = \pi/2$:

$$(4) \qquad d\sigma''/d\Omega = 1/5 \left| A_0(E2) \right|^2, \qquad d\sigma^{\perp}/d\Omega = 1/3 \left| A_0(E1) \right|^2$$

Experimentally this separation can be made by using a target having a spin-zero ground-state and analyzing the energy of the scattered photons to make sure that they popu late only the ground-state. The requirement is that the spectrometer had a resolution good enough to separate the ground-state radiation from that populating the first excited state. Oxigen would not only make the most interesting target, but it is also the easiest to study since its first excited state is at 6 MeV. Other self-conjugate nuclei would also make appropriate targets. Since Bismuth apparently produces no inelastic E1 scattering[19], it might present an opportunity to look for the E2 giant resonance in a heavy nucleus. The experiment would then consist in advancing the incident photon energy through the E1 and E2 giant resonances and measuring $d\sigma''/d\Omega$ and $d\sigma^{\perp}/d\Omega$ simultaneously using a pair of NaI(Tl) detectors. This is a very important experiment since we don't know where or if the E2 strength is in these nuclei.

4.- Compton scattering off nucleons in nuclei (γ, γ'N).-

Above the giant resonance the coherent scattering cross section decreases with increasing energy, while the incoherent Compton scattering (γ, γ'N) by the individuals nucleons becomes important when the incident photon wavelength is comparable to the internu cleon distances. In this process momentum is transferred to the individual nucleons instead of to the whole nucleus and the struck nucleons is emitted. The scattering amplitude is given in the impulse approximation by the product of the Compton scattering amplitude ($\gamma + N \rightarrow \gamma' + N'$) for a nucleon of a particular momentum p and the probability amplitude of finding in the nucleus a nucleon with such momentum p.

This momentum may be determined from momentum conservation if the momenta of the scattered photon and the emitted nucleon are measured. By this method one could mea sure the momentum distribution of nucleons inside nuclei, as in an (e, e'p)-experiment. To achieve this one has to use a monochromatic γ-source and to measure the scattered photon and emitted nucleon in coincidence.

Compared to an (e, e'p)-experiment one would have no problems of radiative tail and radiative corrections. Furthermore, in view of the necessary coincidence experiment the proposed monochromatic photon source would have a much better duty cicle than the available electron sources for (e, e'p).

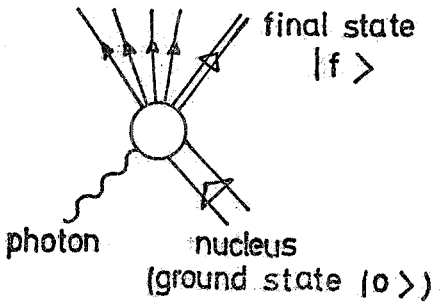

FIG. 9.- Photo-induced nuclear reaction.

III.- PHOTONUCLEON EMISSION PROCESSES.-

Introduction.-

This Chapter will be concerned with the absorption of monoenergetic, real photons of momentum $\underline{k}$ and energy $\omega = |\underline{k}|$ by a complex nucleus, as shown in Fig. 9 leading to a definite final state $|f\rangle$ of the nuclear system, containing one or more nucleons in the continuum. A brief survey and outlook will be given, covering both the major experimental work and the possible theoretical interpretations in this field.

The giant resonance region ($\omega \lesssim 30$ MeV) will be treated very briefly, since a large part of past and present photonuclear activities has been concentrating on such range of energies, and the situation is pretty clear. However, at point 4., there will be a discussion of some sort of additional information which one might obtain by using polarized photons at these energies.

We shall focus mainly on the intermediate energy region (60 MeV$\lesssim \omega \lesssim$140 MeV), which has always been subject to considerable experimental difficulties, a major part of which being related to problems of unfolding the bremsstrahlung yield curves. However, it is expected that the advent of monochromatic (and even polarized) gamma ray sources will stimulate increasing interest in the transition region between the giant resonance and the meson production threshold.

1.- The Giant Resonance Region.-

The understanding of the gross and intermediate structure experimentally observed in the G.R. region has been a major objective of the theoretical efforts in recent years. The fine structure of the dipole states which has been found in several nuclei, for instance via capture reactions, seems however to be at present beyond the possibilities of a complete theoretical description.

The absorption mechanism has been in general described in the framework of the hydrodinamic and of the single particle (plus residual interaction) models. These models may be extended, for example by letting the main dipole excitation to be coupled with other degrees of freedom, such as quadrupole surface oscillations (Dinamic Collective Model).

These approaches have been recently fully discussed in several review articles[6,20,21]; here we only recall that these calculations, by taking some parameters (such as the energy of the transition or the width of the absorption lines) from the experimental observations, have been rather successful to account for most of the intermediate structure in the experimental cross sections. They may be therefore taken as a first basis towards a deeper understanding of the photonuclear processes.

The decay of the G.R. states has been analyzed theoretically by means of several simplifying approaches[6,20,21]: for instance, using the coupled-channel method a reasonable agreement has been obtained for particle widths, but experimental angular distributions and polarization of the photonucleons were not reproduced by the calculations. Actually, angular distributions and polarization are among the measurements which are needed in order to obtain from the reactions information on the nuclear structure aspects of the states involved. Additional information is gained by measuring the azimuthal distributions of photonucleons arising from the absorption of polarized photons. This point will be subsequently discussed (S 4).

On the experimental side, one can observe that the harvest of such more sophisticated data is unfortunately rather poor. The measurements of differential cross sections are obviously more affected by the quality of the photon beam so that, except for a few cases where, for instance, it is possible to isolate ground state transitions, most of the available data are essentially of qualitative importance.

The experiments exploiting the best existing photon beams have been so far essentially devoted to measure total neutron reaction cross sections. The extensive series of measurements carried out at Livermore and Saclay[22] on (γ , γ n) reactions with annihilation photons are in fact the only systematic and self-consistent sets of data with good accuracy available to date.

It can therefore be concluded that accurate experiments are needed both to complete the systematics of reliable total photoreaction cross sections and to put on a quantitative ground the knowledge of differential cross sections.

3.- Photonuclear reactions at intermediate energies.-

At intermediate energies a large variety of fragmentation processes can occur; it is convenient to classify the final states $|f\rangle$ of the nuclear system according to the number of emitted nucleons:

a) one-particle continuum states ((γ , p) and (γ , n) reactions)
b) two-particle continuum states ((γ , pn), (γ , 2p) and (γ , 2n) reactions)
c) composite particle continuum states ((γ , d), (γ , α), etc. reactions).

In this section we shall exclusively concentrate on points a) and b), with special reference to the (γ , pn) process: these are in fact the most important reactions at intermediate energies.

Brief survey of existing experimental data.-

The experimental material pertaining to the photonuclear processes in the intermediate energy region is very scarce. Some effort has been early devoted to estimate the total neutron cross section in a reasonably wide range of target nuclei, but even in this experimentally simpler case the resolution and the accuracy of the results are rather poor.

Some work has also been done with the aim of testing the validity of the "quasi-deuteron" mechanism[23], often in an indirect way[24].

The availability of only Bremsstrahlung beams has, so to say, favoured the use of integral detectors, and the measurements performed at the Lebedeev Institute by Gorbunov and coworkers[23] are particularly important and reliable. Their data give information on some (γ , N) and (γ , 2N) cross sections in light nuclei, such as ^{4}He, ^{12}C and ^{16}O, and on nucleon angular distributions. The low statistical accuracy due to the use of a cloud chamber technique is their major drawback.

Only recently some counter experiments on high energy photonucleon emission from light nuclei have been performed, following more or less the lines of the Whitehead's[26] and Penner-Leiss'[27] pioneer works. In particular, a Glasgow group[28], using an ingenious simple photon difference method, has measured angular distributions of p-shell protons from Lithium isotopes and carbon at some γ-ray energies, and put in evidence the direct emission of fast protons from the s- and p- shells. The direct p-shell photoproton cross section vs. photon energy has been measured for ^{7}Li, ^{9}Be, ^{12}C and ^{16}O in a limited energy range and at a fixed angle by a Genova-Torino group[29]. Similar measurements have been carried out at Saskatoon for neutron emission from ^{12}C[39].

These experiments have evidenced extremely interesting points, and stimulated a lot of fine theoretical work, which will be discussed below.

It will be then clear why it is highly desirable that measurements of this kind be continued and extended possibly using new photon beam facilities allowing the best definition of the initial state.

Kinematical considerations. -

For the photoreactions shown in Fig. 9 , the momentum and energy conservation reads (for a nucleus initially at rest):

$$(5) \qquad \underline{k} = \sum_{\nu=1}^{n} \underline{p}_\nu + \underline{q}_R , \qquad \omega = |\underline{k}| = \sum_{\nu=1}^{n} (p_\nu^2 /2M_\nu + B_\nu) + E_R$$

where the sums extend over a total of n emitted particles, $\underline{p}_\nu$ denotes the (asymptotic) momentum, B_ν the separation energy of the particle ν , $\underline{q}_R$ and E_R the momentum and energy of the residual nucleus.

(γ, N) reactions (n=1) lead to quite pronounced kinematical situations: for $\omega = 100$ MeV, for example, the recoil momentum of the residual nucleus has to be $|\underline{q}_R| \gtrsim 300$ MeV/c (depending on the angle of emission). This is large compared to average momenta of bound nucleons ($\langle p^2 \rangle^{1/2} \sim 100$ MeV/c).

For (γ, pn) reactions (n=2), momentum and energy are shared by the emitted nucleon pair. At $\omega = 100$ MeV, the strong angular correlations involve pn-relative momenta $p_{rel} = 1/2 |\underline{p}_1 - \underline{p}_2|$ of the order of 300 MeV/c, which is again large compared to conventional low energy standards.

Photonuclear cross sections. -

If the basic photonuclear interaction is considered the coupling of the photon to pointlike nucleons with currents $e\underline{p}/M$ and magnetic moments $e\mu\sigma/2M$, the cross section for the photon induced transition to a definite final state $|f\rangle$ can be written (in units of h=c=1, $e^2 = 1/137$) as:

$$(6) \qquad \sigma_{fo}(\omega) = 4\pi^2 e^2 \omega^{-1} |\langle f| \hat{\varepsilon} \left[\underline{J}(\underline{k}) + i\underline{M}(\underline{k}) \right] |0\rangle|^2 \varrho_f(\omega) ,$$

where $\underline{J}$ and $\underline{M}$ are the nuclear current and magnetic moment contributions:

$$(7) \qquad \underline{J}(\underline{k}) = \sum_{j=1}^{A} \frac{1+\tau_3(j)}{2} \frac{\underline{P}_j}{M} \exp(i\underline{k} \cdot \underline{r}_j)$$

$$(8) \qquad \underline{M}(\underline{k}) = \sum_{j=1}^{A} \frac{\mu_j}{2M} (\underline{k} \times \underline{\sigma}_j) \exp(i\underline{k} \cdot \underline{r}_j) ,$$

$\hat{\varepsilon}$ denotes the photon polarization vector, and ϱ_f is the density of final states. Modifications to the simple picture represented by eqs. (7) and (8), which only takes into account the basic one-body N-vertex shown in Fig. 10, will be discussed later.

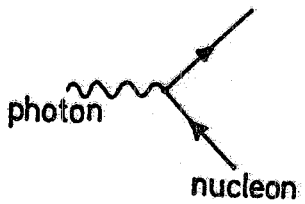

FIG. 10 - The basic one-body N-vertex.

Nuclear models. -

Model calculations of the photonuclear cross sections of eq. (6) require the specification of the nuclear states $|0\rangle$ and $|f\rangle$. According to the kinematical considerations mentioned above, it is expected that conventional nuclear models developed to explain low energy nuclear data will hardly be able to describe the intermediate energy phenomena within the given frame of eqs. (6) ÷ (8).

A. -The Independent Particle Model (IPM). -

Within the IPM, the wave functions of the nuclear initial and final states, $\Phi_o(1, \ldots, A)$ and $\Phi_f(1, \ldots, A)$ are Slater determinants of single particle wave functions, obtained as solu-

tions of a one-body Schrodinger equation, with, for example, a Woods-Saxon optical potential. Since $\underline{J}$ and $\underline{M}$ of eqs. (7) and (8) are one-body operators, only single nucleon emission processes can be described on the basis of the IPM[30]. Realistic calculations in the IPM show that (γ, p) cross sections systematically come out too small, indicating that the conventional shell model does not provide considerably large single particle momenta with sufficient probability. Furthermore, (γ, n) reactions only emerge via the magnetic coupling of eq. (8), which is relatively small; consequently, in the IPM picture, (γ, n) cross sections are generally underestimated by orders of magnitude.

It should be noted, however, that these considerations have disregarded the fact that the IPM wave function is not translationally invariant. For instance, this is important for E1 transitions, where the Gartenhaus-Schwartz transformation yields an effective electric charge -Z/A for the neutrons, thus making E1 transitions in (γ, n) processes possible.

B. -Correlations in Nuclei and the Jastrow Model. -

Both the dominance of the (γ, pn) reaction, and the observed probability of finding rather high Fourier components in the nuclear wave functions for (γ, N) processes indicate the relevance of two-nucleon mechanism in intermediate energy photoabsorption. Levinger was the first to point out that the absorption process might involve deuteron-like substructures (quasi-deuteron model[31], developed further by several authors[32]). In this picture the (γ, pn) cross section is related to the cross section for deuteron photodisintegration by

$$\sigma_{(\gamma, pn)} = L \frac{NZ}{A} \sigma_{(\gamma d \rightarrow pn)} \tag{9}$$

where the factor L is theoretically estimated to be 6.4: experimentally, L turns out to be energy dependent and its value ranges between about 4 and 10.

The effects of relatively short range correlations in nuclei can be treated, among other methods, within the frame of the Jastrow model: the IPM wave function $\Phi(1, \ldots, A)$ is modified by nucleon pair correlation factors f(ij) to obtain the correlated A-body wave function ψ:

$$\psi(1, \ldots, A) = F\Phi(1, \ldots, A), \qquad F = \prod_{i<j} f(ij) \tag{10}$$

The matrix elements of the one-body operators $\underline{J}$ and $\underline{M}$ of eq. (6) are now given by

$$\langle \psi_f | \hat{\varepsilon}_\bullet (\underline{J} + i\underline{M}) | \psi_o \rangle = \langle \Phi_f | \hat{\varepsilon}_\bullet (\underline{J}_{eff} + i\underline{M}_{eff}) | \Phi_o \rangle \tag{11}$$

$$\underline{J}_{eff} = F^+ \underline{J} F, \qquad \underline{M}_{eff} = F^+ \underline{M} F \tag{12}$$

where $\underline{J}_{eff}$ and $\underline{M}_{eff}$ are many-body operators acting on IPM wave functions.

In the phenomenological approach towards Jastrow correlations, the two nucleon correlation factors f(ij) are conveniently parametrized in terms of the relative momentum q_c exchanged between pairs of independently moving nucleons. The Jastrow model has been applied to both (γ, pn) and (γ, N) reactions[33] and seems to account quite well for some general features (orders of magnitude of cross sections, shapes of angular distributions) of these processes. However, the correlation factors used so far do not seem to be related to any so called realistic nucleon-nucleon potential[34].

As an example, Figs. 11 ÷ 13 show a recent Jastrow model analysis of (γ, p) differential cross sections[35].

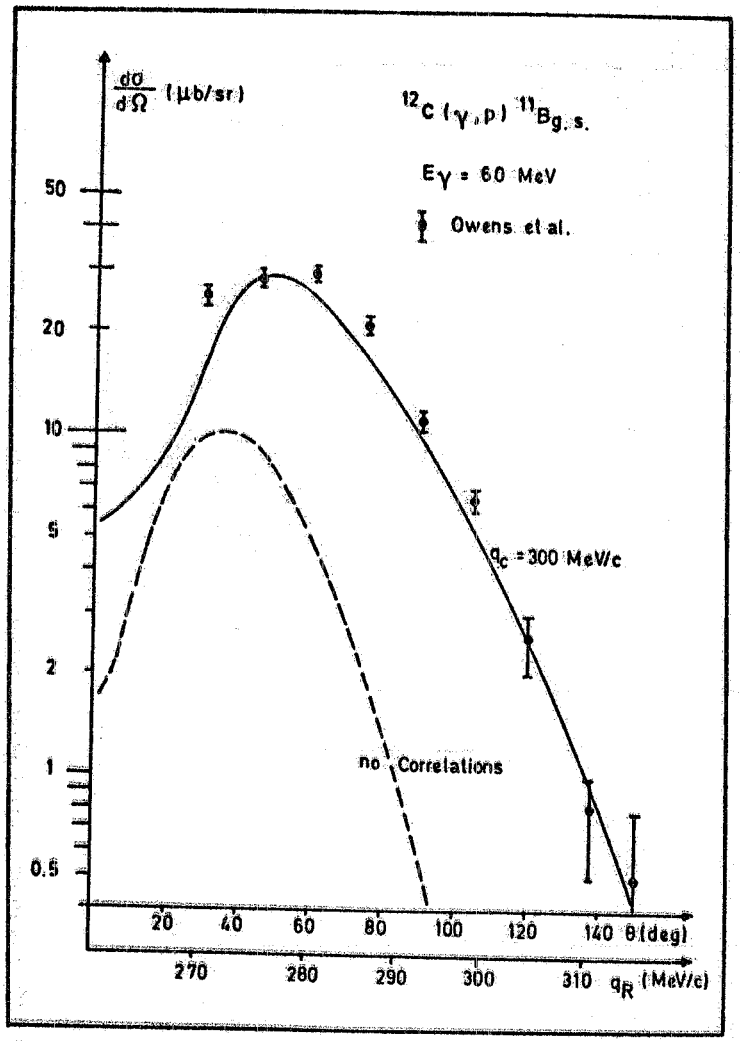

FIG. 11 - Jastrow model analysis of $^{12}C(\gamma, p)$ differential cross section for emission of p-shell protons at photon energy $E_\gamma = 60$ MeV. q_R is the recoil momentum of the residual nucleus. Both curves (with and without correlations) include realistic distorsions of the outgoing proton (complex optical potential). q_c is the correlation parameter, i.e. the relative momentum to be exchanged between otherwise independently moving nucleons.

Generally, the Jastrow approach seems to be rather successful in correlating a large variety of intermediate energy data, although - at its present stage - it does not offer any further microscopic insight into the basic absorption mechanism. In this context, high precision experiments with monochromatic photon beams might well stimulate further developments of the model, as well as examination of its possible limits of applicability.

Mesonic degrees of freedom in photon interactions. -

Up to now, the discussion has always been moving within the conventional frame of photons interacting with currents created exclusively by point like nucleons. This has led to the one-body interaction operators of eqs. (6) and (7), which correspond to the basic N-vertex of Fig. 10. However, it is in fact well known that there exists quite different interaction mechanism, related to currents of charged mesons in the nucleus. The basic coupling of the photon to these mesonic degrees of freedom is a very familiar phenomenon beyond the meson production threshold, where the photoproduction of π-mesons becomes the dominant reaction channel (see Fig. 14). In nuclei, the same sort of mechanism can of course take place virtually below threshold, the photo-produced virtual pion being absorbed by a second nearby nucleon, as shown in Fig. 15.

To the lowest order in the coupling constants, the exchange current contribution of Fig. 15 is represented by the diagrams of Fig. 16. Their non-relativistic reduction yields two-body operators for the current terms, corresponding to the diagrams a) and b) of Fig. 16 respectively:

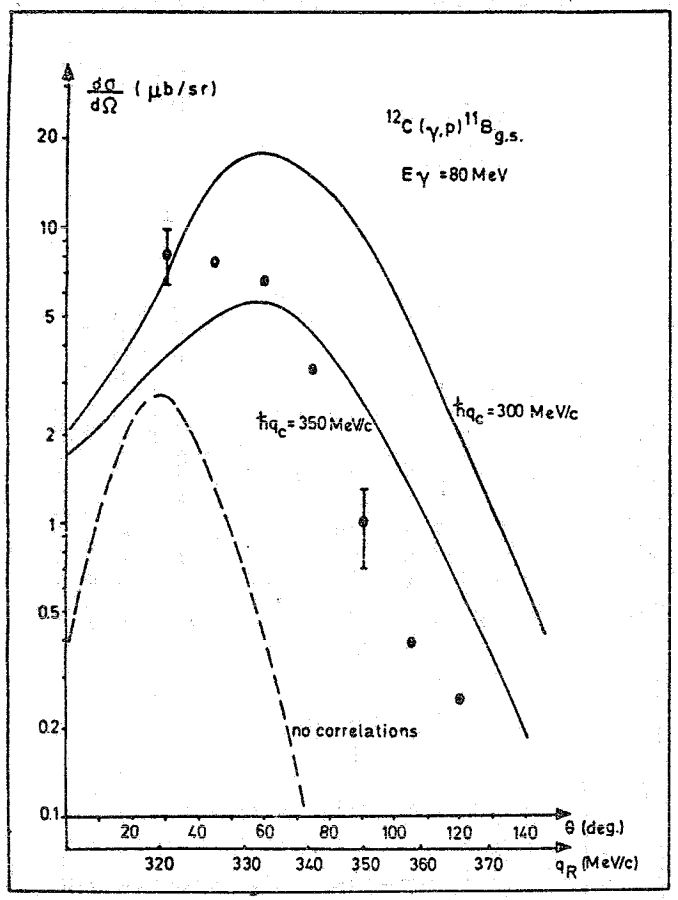

FIG. 12

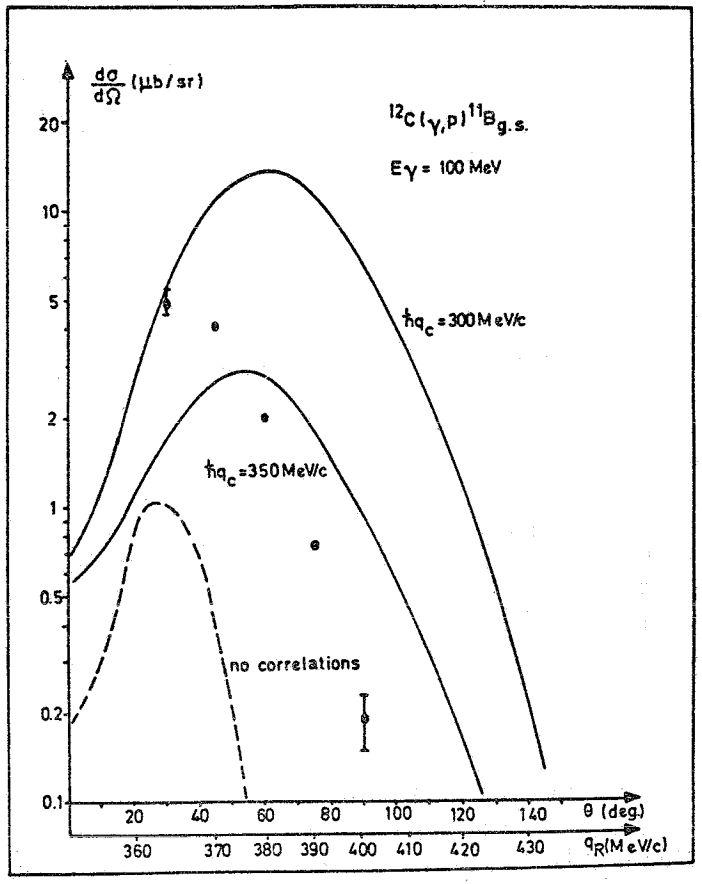

FIG. 13

FIG. 12 and 13: As Fig. 1, for $E_\gamma = 80$ MeV and $E_\gamma = 100$ MeV. Experimental data: Owens et al.

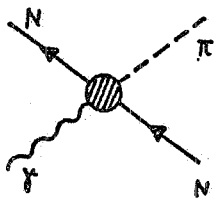

FIG. 14 - Photoproduction of π mesons.

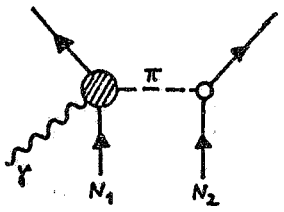

FIG. 15 - Exchange current contribution to nuclear photo absorption.

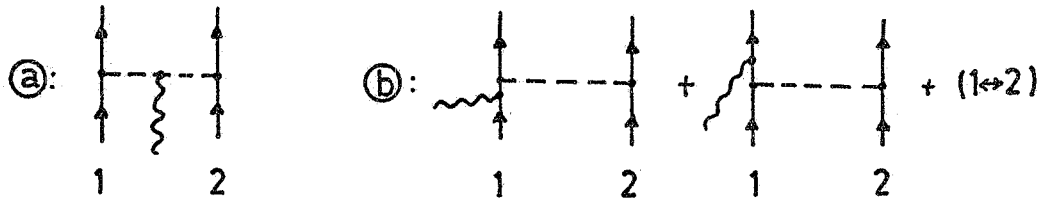

FIG. 16 - Exchange current contributions in lowest order.

$$\underline{J}^{(2)}_{\pi}(\underline{k}) = \frac{1}{4\pi}\left(\frac{G}{2M}\right)^2 \sum_{i<j} \left[\underline{\tau}(i)\times\underline{\tau}(j)\right]_{\zeta} (\underline{\sigma}_i\cdot\underline{\nabla}_i)(\underline{\sigma}_j\cdot\underline{\nabla}_j)\,\underline{r}_{ij}\,\frac{e^{-m r_{ij}}}{r_{ij}} \times$$

$$\times \int_0^1 d\alpha \exp\left\{i\underline{k}\cdot\left[(1-\alpha)\underline{r}_i + \alpha\,\underline{r}_j\right]\right\} \tag{13 a}$$

$$\underline{J}^{(2)}_{N}(\underline{k}) = -\frac{1}{4\pi}\left(\frac{G}{2M}\right)^2 \sum_{i<j} \left[\underline{\tau}(i)\times\underline{\tau}(j)\right]_{\zeta}\cdot\left[(\underline{\sigma}_i\cdot\underline{r}_{ij})\,\underline{\sigma}_j\, e^{i\underline{k}\cdot\underline{r}_j} + \right.$$

$$\left. + (\underline{\sigma}_j\cdot\underline{r}_{ij})\underline{\sigma}_i\, e^{i\underline{k}\cdot\underline{r}_i}\right]\left(1+\frac{1}{m r_{ij}}\right)\frac{e^{-m r_{ij}}}{r_{ij}} \tag{13 b}$$

Here m is the pion mass, G is the pion-nucleon coupling constant, and $r_{ij}=|\underline{r}_i-\underline{r}_j|$. Clearly, these operators introduce a sort of two-nucleon interaction mechanism, which seems to be a basic feature of intermediate energy photoabsorption. These effects cannot be given by the Jastrow model, they are a specific property of the electromagnetic interaction with pionic degrees of freedom in nuclei. The total current operator $\underline{J}$ in eq. (6) now consists of a one-body and a two-body part:

$$\underline{J}(\underline{k}) = \underline{J}^{(1)}(\underline{k}) + \underline{J}^{(2)}(\underline{k}) \tag{14}$$

where $\underline{J}^{(1)}(\underline{k})$ is the conventional term of eq. (7), and

(15) $$\underline{J}^{(2)}(\underline{k}) = \underline{J}_{\pi}^{(2)}(\underline{k}) + \underline{J}_{N}^{(2)}(\underline{k})$$

Calculations of photonuclear cross sections along these lines have not yet been carried out. Estimates of exchange current contributions to the dipole sum rule[36] seem to indicate that these effects are by no means small. Furthermore eq. (13) shows that the two-body terms are highly symmetric with respect to the two participating nucleons, which might help to understand the observed similarity between (γ, p) and (γ, n) differential cross sections. In fact, if the two-particle absorption mechanism would exclusively be due to the current of eq. (15), then the (γ, p) and (γ, n) cross sections would be completely equal.

4.- Reactions with polarized photons.-

Plane polarized photons beams may give additional information over that obtainable with unpolarized beams of the same characteristics. The formalism to use in considering experiments with polarized photons, and a general discussion on such experiments are presented in a paper by Satchler[37] and in the monograph by Hayward[6]; some applications can be found in ref. (18).

Consider the angular distribution of single nucleons emitted after the absorption of photons of a given energy ω=k. For unpolarized photons the angular distribution may be represented by the familiar Legendre expansion

(16) $$I(\theta;k) = \sum_{\nu LL'} A_{\nu}(LL';k)\ P_{\nu}(\cos\theta)$$

where θ is the nucleon emission angle and L, L' explicitely refer to the photon multipolarities involved in the transition. For plane polarized photons, eq. (16) is to be replaced by

(17) $$I(\theta,\varphi;k) = \sum_{\nu LL'} A_{\nu}(LL';k)\ F_{\nu}^{LL'}(\theta,\varphi)$$

where

(18) $$F_{\nu}^{LL'}(\theta,\varphi) = P_{\nu}(\cos\theta) + p\,\varkappa_{L'}\, f_{\nu}(LL')\cos 2\varphi\, P^{2}(\cos\theta)$$

Here $\varkappa_{L'}$=+1 or -1 depending on whether the multipole L' is electric or magnetic, respectively. The degree of polarization of the photon beam is denoted by p; the $P^2(\cos\theta)$ are associate Legendre polinomials, and φ is the azimuthal angle between the photon polarization vector and the reaction plane. The geometrical coefficients $f_{\nu}(LL')$ are given by

(19) $$f_{\nu}(LL') = -\sqrt{\frac{(\nu-2)!}{(\nu+2)!}}\ \frac{\begin{pmatrix} L & L' & \nu \\ 1 & 1 & -2 \end{pmatrix}}{\begin{pmatrix} L & L' & \nu \\ 1 & -1 & 0 \end{pmatrix}}$$

A few specific values of these functions and coefficients are listed in Table IIb.

Quantities of special interest are the counting rates parallel and perpendicular to the plane of photon polarization, $I^{\parallel}$ and $I^{\perp}$, given by

(20) $$I^{\parallel}(\theta;k) = I(\theta,\varphi=0;k), \qquad I^{\perp}(\theta;k) = I(\theta,\varphi=\frac{\pi}{2};k)$$

The asymmetry $A(\theta;k)$ is defined by

(21) $$A(\theta;k) = \frac{I^{\perp}(\theta;k) - I''(\theta;k)}{I^{\perp}(\theta;k) + I''(\theta;k)}$$

If only electric dipole transition occur, as it does in the Giant Resonance, then the angular distributions of nucleons are symmetric about 90^{o} and the use of polarized photons does not add new information, but it allows a much more sensitive determination of the angular distribution parameters. But if, on the other hand, the angular distributions are asymmetric, indicating a E1-M1 or a E1-E2 interference, then a measurement using polarized photons allows the distinction to be made.

Appendices A, B and C present some examples of additional sensitivity gained in polarization experiment at lower energies:

a) Determination of angular coefficients (Appendix A)
b) Parity assignments in dipole transitions (Appendix B)
c) Angular distribution in E1-E2 interference (Appendix C).

In addition, the E2-photodisintegration of ^{4}He into a pair of deuterons is discussed in Appendix D.

At intermediate energies, the measurement of asymmetries $A(\theta)$ for processes like (γ, N) is expected to yield an additional sort of information beyond that obtained from the unpolarized differential cross sections. The comparison of $A(\theta)$ for (γ, p) and (γ, n) reactions, for example, could provide a sensitive tool to study how far the similarities between such reactions really go: as stated previously at point 3, this might be of considerable interest for detailed discussions of the two-body absorption mechanism at photon energies around 100 MeV.

In that context, it would also be interesting to compare the asymmetries of (γ, pn) differential cross sections to those observed in the photodisintegration of the deuteron. If, for example, the original quasideuteron model is assumed to hold, these asymmetries should be equal.

Furthermore, it should be remarked that polarized photons experiments may contribute to the question about possible contributions of long range correlations (collective excitations) to the direct two-body absorption process discussed at point 3.

IV. - THE PHOTODISINTEGRATION OF THE DEUTERON USING LINEARLY POLARIZED PHOTONS. -

Some time ago De Swart and Marshak[41] proposed that the photodisintegration of the deuteron be studied using linearly polarized photons to determine the contribution of the M1 spin-flip amplitudes to the total cross section. They suggested that this be done at 80 MeV. Since that time a much more exhausting study of the deuteron photodisintegration has been made by Partovi[42], in which he includes multipoles up to L=3 and treats the problem in a series of Approximations A through I, each more sophisticated than the one before.

For linearly polarized photons Partovi writes the angular distribution

(22) $$d\sigma/d\Omega = I_{o}(\theta)\left[1 + p\ \Sigma(\theta)\cos 2\varphi\right]$$

where p is the degree of linear polarization and φ is the angle between the plane of linear polarization and the azimuthal angle of observation; the function $I_{o}(\theta)$ and $\Sigma(\theta)$ are given in Partovi's paper.

In an experiment one measures the asymmetry given by (21) that may be written also

(22) $$A(\theta;k) = \frac{d\sigma^{\perp} - d\sigma''}{d\sigma^{\perp} + d\sigma''} = -p\ \Sigma(\theta)$$

If the polarization is complete then (22) gives

(23) $$A(\theta;k) = -\Sigma(\theta)$$

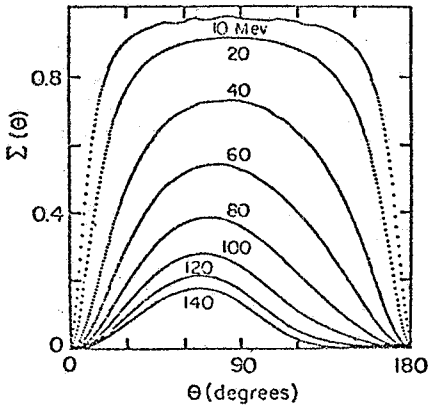

FIG. 17

Fig. 17 shows a plot of $\Sigma(\theta)$ as a function of θ for different energies in Approximations I. Fig. 18 shows $\Sigma(\pi/2)$ as a function of energy in Approximations E and I.

In the photon energy range 75 to 230 MeV the deuteron photodisintegration has been studied[43] using polarized bremsstrahlung. Up to 140 MeV his results agree much better with Approximation E than with Approximation I. If we can believe both the experiment and the Partovi calculation, the effects of meson currents and nucleon polarization[44] need to be included for photon energies as low as 100 MeV. This experiment is of sufficient importance that it should be repeated.

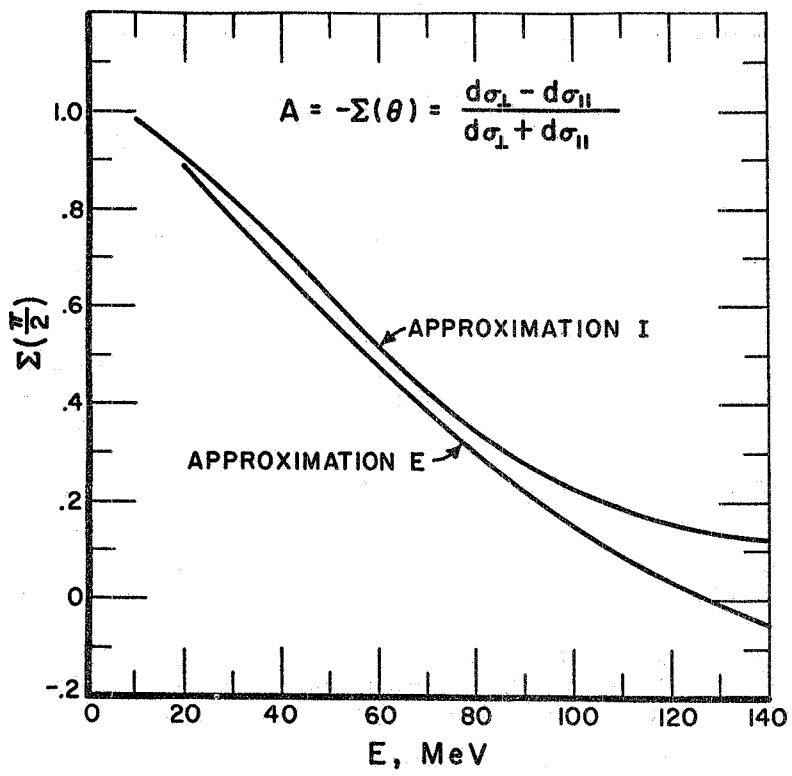

FIG. 18

V. - ACTIVATION METHODS FOR PARTIAL CROSS SECTION MEASUREMENTS. -

When one starts to do a new kind of physics, it is always a good idea to make a survey, i.e., to measure the same quantities for a range of nuclides. For instance, if it is known that the photon beam is monochromatic, then it is an excellent idea to measure (γ, n), (γ, p), and (γ, pn) cross section magnitudes as a function of energy using activation techniques. Select targets in which the radioactivities generated have reasonable half-lives and where the reactions studied can be easily separated from other mechanisms by γ-ray spectroscopy. In this way one avoids all the problems connected with the dependence of detector

efficiency on nucleon energy or molteplicity. A specific cross section can be measured. These experiments also have the advantage that a high photon flux is not required since the detector-target is placed in the photon beams. To have such cross sections measured over a wide range of A values may show some very interesting trends.

For example, the quasi deuteron absorption mechanism is thought to be the dominant one on the energy range 50-100 MeV. It is therefore very important to measure the (γ, pn) cross sections because of their relationship to this mechanism. The (γ, pn) process results in many measurable radioactivities with convenient half-lives and producing X-rays that can be counted using high resolution Ge(Li) detectors. As the nuclear volume increases, the chance that one of the nucleons will interact before emerging becomes greater. These interactions result in the emission of two, three, four, or even more nucleons. Again, in many cases these reactions produce measurable radioactivities so that one could determine with monochromatic photons the cross section for the emission of, say, three neutrons. For example, the relative integrated cross sections have been measured[45] for the production of twelve different radioactivities when ^{209}Bi was exposed to 137 MeV Bremsstrahlung. These were produced in exotic reactions such as $^{209}Bi(\gamma, 9n)$, $^{209}Bi(\gamma, 6np)$, etc. It would be very interesting to have these cross sections measured absolutely and as a function of energy.

VI. - FINAL REMARKS. -

Table I clearly indicates the distinct features of our proposed photon facility: complete absence of low energy photons in the beam and linear polarization close to 100%. These features will allow some series of experiments which have not been possible up to now or have yielded inconclusive results. We would like to discuss here a few categories:

1) Inclusive reactions induced by high energy photons in which low energy particles are detected,
2) photoreactions with polarized photons,
3) coherent and incoherent scattering of polarized photons on nuclei.

1. - Inclusive reactions. -

The most common inclusive reactions in nuclear physics are the (γ, n) and $(\gamma, 2n)$ reactions. Extensive measurements of these cross sections have been made with Bremsstrahlung beams and more recently with monoenergetic photons obtained from positron annihilation in flight. However, most of the existing measurements are limited to gamma ray energies lower than 30 or 40 MeV. At higher energies the neutrons produced by the lower energy photons present in the beams constitute a very large background making the experiment more difficult and the statistical error much larger. A monochromatic photon beam without low energy tail could easily extend the existing measurements to its highest energy with traditional detectors. Let us assume that we use a 4π thermalized neutron detector with an efficiency of 20%, a target thickness of approximately 0.01 radiation lengths and a beam intensity of 10^7 photons per second. In this condition the counting rate ν is given in the last column of Table III. The nucleus under consideration is indicated in the first column, the assumed total photoneutron cross section in the second column and the target thickness (nuclei/cm^2) in the third column.

TABLE III

Nucleus	σ_{TOT} cm^2	N Nuclei/cm^2	ν Counts/Hour
^4He	5×10^{-29}	1.3×10^{23}	47.000
^{63}Cu	5×10^{-28}	1.13×10^{21}	4.000
^{209}Bi	2×10^{-27}	1.9×10^{20}	3.000

2.- Photoreactions.-

High energy photoreactions with the emission of a single nucleon were shown to be a sensitive test of nuclear models. Polarized photons, with an extra degree of freedom, increase the sensitivity to nuclear models and can reveal contributions from higher multipoles. The study of the cross section for the direct reactions (γ, p) and (γ, n) is made difficult by the small size of the cross section. In the (γ, p) measurements, moreover, the target thickness is limited by the requirement to keep the energy loss in the target of the outgoing proton small and compatible with the required energy resolution.

In Table IV we have collected some tentative numbers for the study of the reaction $O^{16}(\gamma, p)N^{15*}$. In the first two columns are indicated the gamma ray energy and the corresponding proton resonance energy; the maximum energy loss allowed in the target is in column 3, in column 5 the corresponding target thickness expressed in nuclei/cm^2, and in column 6 the assumed value of the cross section. The estimated counting rates, for a solid angle $\Delta\Omega = 0.1$ sr, are in the last column.

TABLE IV

K MeV	E MeV	ΔE MeV	ΔX gr/cm^2	N Nuclei/cm^2	$d\sigma/d\Omega$ cm^2/sr	ν Counts/Hour
50	35	1	0.067	2.5×10^{21}	4×10^{-29}	360
60	45	13	0.104	3.9×10^{21}	2×10^{-29}	280
80	65	2	0.218	8.2×10^{21}	5×10^{-28}	150

To discuss the feasibility of the study of the reactions (γ, n) at high energy we will consider the specific process $C^{12}(\gamma, n)C^{11}$ for which some measurements already exist at gamma ray energies between 64 and 123 MeV[47]. At a gamma ray energy of 83 MeV we have a resonance neutron energy of 58 MeV and a differential cross section, integrated over the neutron resonance, of approximately 10 μb/sr at 40° in the Laboratory System. Let us assume that we use a large neutron detector of $30 \times 30 \times 20$ cm^3 located at 3 m from the target with an overall neutron detection efficiency (ε) of 10% and covering a solid angle ($\Delta\Omega$) of 10^{-2} sr. In these conditions with a target thickness of 4 gr/cm^2 (approximately 0.1 radiation length) and our beam intensity of 10^7 photons/sec we obtain a counting rate of 72 counts/hour. The energy of the outgoing neutron must be measured by time of flight technique. Its resolution is determined by the length of the flight path and the time resolution of the apparatus. In the storage ring Adone electrons travel in bunches not longer than 40 cm. The monochromatic photons have the same time structure due to the production mechanism. Therefore, the electron bunches can be used as a start signal for the time of flight circuitry. The stop signal is provided by the neutron counter itself. With our parameters the time resolution of the neutron detector should be smaller than that of the electron bunches. With all this in mind we can now calculate:

$$\frac{\Delta E}{E} = 2\frac{\Delta v}{v} = 2\frac{\Delta t}{t} = 2\Delta t\frac{c\beta}{l} = \frac{2 \times 1.5 \times 10^{-9} \times 3 \times 10^{8} \times 0.32}{3} = 0.096$$

or:

$$\Delta E \simeq 4.6 \text{ MeV}$$

The width of the neutron resonance being approximately 10 MeV, a neutron energy resolution better than 5 MeV is perfectly acceptable.

3.- Photon scattering.-

Photon scattering by the giant resonance of nuclei and Delbrück scattering will be discussed in this paragraph. These processes contribute to the same cross section. Therefore

the different angular distributions must be used to separate the two contributions. Delbrück scattering is strongly peaked forward while the angular dependence of nuclear scattering is characterized by a second degree polinomial in $\cos\theta$.

a) - Delbrück Scattering. -

At an energy of 80 MeV the most interesting region for Delbrück scattering is at small angles, where the momentum transfer is comparable or larger than the electron mass, and most approximations are not valid. In Table V we have indicated, for some typical values of the momentum transfer, the theoretical values of the differential cross section calculated for Pb at a gamma ray energy of 80 MeV[12], the solid angle which can reasonably be used at each angle ($\Delta\Omega \approx \theta^2$) and the expected counting rate in the last column.

TABLE V

Δ MeV	$\pi\, d\sigma/dt$ $\mu b/GeV^2$	$d\sigma/d\Omega$ mb/sr	θ rad.	$\Delta\Omega$ sr	$(d\sigma/d\Omega)\Delta\Omega$ mb	ν counts/hour
0.4	80	24.000	0.005	2.10^{-5}	0.48	3300
1	12	3.600	0.0125	2.10^{-4}	0.72	4900
2	1.5	4.50	0.025	6.10^{-4}	0.27	1850
5	0.1	29	0.0625	4.10^{-3}	0.12	820
10	0.01	2.9	0.125	10^{-2}	0.03	205

These values have been obtained for a target thickness of 0.0652 gr/cm^2 equivalent to 1% of a radiation length.

b) - Nuclear scattering. -

Only one experiment of nuclear scattering of plane polarized photons has been published up to now[18]. This was done at a gamma ray energy of 15.1 MeV. We have assumed to work at the same energy and have used some approximate values of the cross sections reported in Table III of that paper. We have also assumed to measure the scattering at 90° in the Laboratory System and to use a target thickness of one tenth of a radiation length. With this hypothesis, for three different elements the counting rate is given in the last column of Table VI.

TABLE VI

Nucleus	$\lvert A_o\rvert^2$ mb	$d\sigma(90°)/d\Omega$ mb/sr	N nuclei/cm^2	ν counts/hour
Sn	0.82	0.14	4.5×10^{21}	2400
W	2.05	0.34	2.25×10^{21}	2750
Bi	3.43	0.57	1.90×10^{21}	3800

SUMMARY. -

There exists at present the concrete possibility of realizing a facility which gives almost completely polarized ($p \geq 98\%$) and even quasi-monochromatic photons up to about 100 MeV.

The importance of the proposed beam for future photonuclear work is underlined, for instance, by the following arguments:

i) Delbrück scattering can be favourably studied by taking into account the dependence of the scattering amplitude on photon polarization;

ii) nuclear coherent and incoherent scattering can be easily separated in E1 approximation, or, conversely, the multipolarities E1 or E2 can be unambiguously assigned to coherent scattering of polarized photons;

iii) monochromatic photons, without lower energy background, are the best tool for studying incoherent Compton scattering on bound protons;

iv) in photonucleons emission processes, a polarized photon beam is extremely helpful in obtaining an increment of sensitivity in the extraction of angular distribution coefficients and in the quantitative analysis of interfering multipoles. In particular, very clarifying is the study of the deuteron photodisintegration with polarized photons;

v) in the intermediate energy region (above the GDR) where experimental material is very scarce, monochromatic and polarized photons are an extremely useful and sensitive tool for precise and detailed measurements of (γ, n) and (γ, p) reactions, which are of crucial importance for the theory;

vi) multinucleon final states can be studied in detail for the first time exploiting the high duty factor of the proposed facility, thus checking, by the polarization effect, nuclear models to a greater precision.

The physics involved in such experiments was subjected to a detailed discussion, implemented in some cases by a first evaluation of the counting rate which can be expected by using the proposed beam. I all the cases studied, data with good statistical accuracy can be obtained in reasonable times.

APPENDIX A - Determination of Angular Distribution Coefficients in E1-Transitions. -

In the giant resonance region, E1-transitions are by far dominating. In this case, we have $\nu = 0$ and 2 only, $L = L' = 1$ and $\varkappa_{L'} = +1$, which leads to

(A1) $$I(\theta,\varphi) = A_0 P_0 + A_2 \left\{ P_2(\cos\theta) - \frac{3}{2} p \sin^2\theta \cos^2\varphi \right\}$$

For 100% polarization (p=1), one obtains, for example:

(A2) $$I''(\theta=\frac{1}{2}\pi) = A_0 - 2A_2, \qquad I^{\perp}(\theta=\frac{1}{2}\pi) = A_0 + A_2$$

The 90°-asymmetry is given by

(A3) $$A(\theta=\frac{1}{2}\pi) = 3A_2/(2A_0 - A_2)$$

The quantity of interest, namely the ratio A_2/A_0, can of course be obtained by directly analyzing the angular distribution (without polarization). However, a considerable increase in sensitivity is gained with polarized photons. This is shown in Fig. 19. In addition, Figure 20 gives the sensitivity as a function of the degree of polarization for a given ratio A_2/A_0, showing that it is essential to work with as large a value of p as possible.

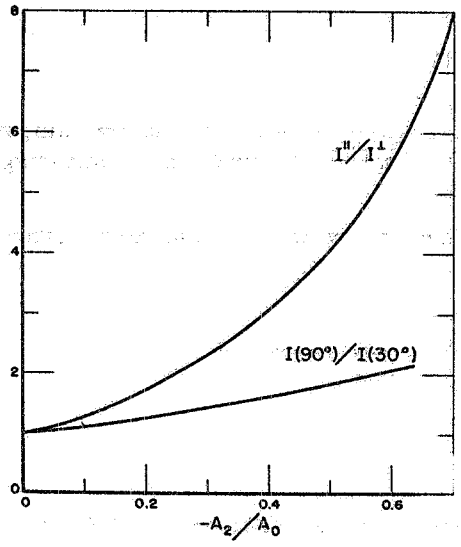

FIG. 19 - Sensitivity for determination of A_2/A_0 with polarized and unpolarized photons. The ratios $I''/I^{\perp}$ refer to the polarized measurement, p denotes the degree of polarization. $I(90^\circ)/I(30^\circ)$ is the result for a typical unpolarized measurement.

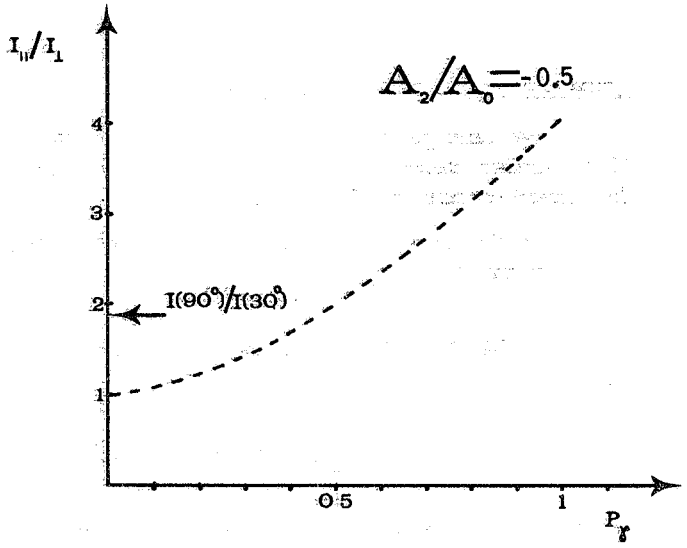

FIG. 20 - Value of $I_{\parallel}/I_{\perp}$ as a function of the degree of polarization of the photon beam for $A_2/A_0 = -0.5$.

APPENDIX B - Parity Assignements: E1-M1 - Mixture. -

If there is a mixture of E1 and M1 radiation encountered, one has (for p = 1):

(B1) $$I(\theta,\varphi) = a_0 P_0 + a_1 P_1(\cos\theta) + a_2 P_2(\cos\theta) - 3/2\, b_2 \sin^2\theta \cos 2\varphi$$

The a_ν and b_2 are sums of $A_\nu(LL')$ of eq. (16) over different combinations of electric and

magnetic dipoles. The important point is that:

$$a_2 = A_2^E + A_2^M, \qquad b_2 = A_2^E - A_2^M \tag{B 2}$$

where:

$$A_2^E = A_2(E1, E1), \qquad A_2^M = A_2(M1, M1)$$

So that there is a chance to separate the E1- and M1- components A_2^E and A_2^M, or, equivalently, to assign parities to the dipole radiation involved. For example:

$$\begin{aligned} I''(\theta = \tfrac{1}{2}\pi) &= a_o - \tfrac{1}{2}(A_2^E + A_2^M) - 3/2\,(A_2^E - A_2^M) \\ I^{\perp}(\theta = \tfrac{\pi}{2}) &= a_o - \tfrac{1}{2}(A_2^E + A_2^M) + 3/2\,(A_2^E - A_2^M) \end{aligned} \tag{B 3}$$

The 90^o asymmetry is given by

$$A(\theta = \tfrac{\pi}{2}) = \frac{3(A_2^E - A_2^M)}{2a_o - A_2^E - A_2^M} \tag{B 4}$$

APPENDIX C - E1 - E2- Mixtures. -

At energies beyond the giant resonance, higher multipoles start to become important. The angular distribution of emitted photonucleons tends to forward directions, indicating the interference of E1 transitions with higher multipoles.

In the case of E1-E2-mixing, the angular distribution, including total polarization (p=1), becomes:

$$\begin{aligned} I(\theta, \varphi) = {} & \sum_{o}^{4} a_i P_i(\cos\theta) - \frac{3}{2} b_2 \cos 2\varphi \sin^2\theta - \frac{15}{6} a_3 \cos 2\varphi \cos\theta \sin^2\theta - \\ & - \frac{15}{24} a_4 \cos 2\varphi \sin^2\theta (7\cos^2\theta - 1) \end{aligned} \tag{C 1}$$

where the coefficients a_i and b_2 are expressed in terms of the $A_\nu(LL')$ of eq. (16) by

$$\begin{aligned} & a_o = A_o(11) + A_o(22); \quad a_1 = A_1(12) + A_1(21); \quad a_2 = A_2(11) + A_2(22), \quad b_2 = A_2(11) - A_2(22); \\ & a_3 = A_3(12) + A_3(21); \quad a_4 = A_4(22) \end{aligned} \tag{C 2}$$

Thus measurements of $I^{\perp}(\theta)$ and $I''(\theta)$ at, for example, $\theta = 45^o$ and $\theta = 135^o$ lead to an increase of sensitivity in determing the angular distribution coefficients.

APPENDIX D - The E2-photodisintegration of ^{4}He into a pair of deuterons. -

The photodisintegration of ^{4}He into two deuterons at low energy, ^{4}He$(\gamma, d)d$, is the only known pure E2 cross section[46] in photonuclear reactions. The angular distribution is well-known to vary as $\sin^2\theta \cos^2\theta$. Expressed in terms of the Legendre functions this becomes:

(D 1) $$I(\theta) = P_o + \frac{5}{7} P_2(\cos\theta) - \frac{12}{7} P_4(\cos\theta)$$

If plane polarized photons are used, then this becomes

(D 2) $$I(\theta,\varphi) = 5 + \frac{5}{7}\left[\frac{1}{2}(3\cos^2\theta - 1) + \frac{3}{2}\sin^2\theta\cos 2\varphi\right] -$$
$$- \frac{12}{7}\left[\frac{1}{8}(35\cos^4\theta - 30\cos^2\theta + 3) - \frac{5}{8}\sin^2\theta\,(7\cos^2\theta - 1)\cos 2\varphi\right]$$

which simplifies to

(D 3) $$I(\theta,\varphi) = \frac{25}{2}\sin^2\theta\cos^2\theta(1+\cos 2\varphi), \qquad I''(\theta) = 25\sin^2\theta\cos^2\theta), \qquad I^{\perp}(\theta) = 0$$

and the asymmetry is $A = -1$.

Given sufficient plane polarized beam intensity to study this reaction, it can be used to determine the degree of polarization of the beam. In fact, any intensity in the direction perpendicular to the polarization vector, $I^{\perp}(\theta)$, measures the effects of finite solid angle and the incomplete polarization in the incident beam.

At higher energies, the same reaction can be used to investigate the contributions of multipoles different from E2, which should show up in $I^{\perp}(\theta) \neq 0$.

REFERENCES. -

(1) - F.R. Arutyunyan and V.A. Tumanyan, Phys. Letters 4, 177 (1963); Soviet Phys.-Uspekhi 83, 339 (1964).
(2) - C. Pellegrini, Parametri di Adone, Struttura dei fasci e luminosità, Frascati Internal Report LNF-67/46(Int.) (1967).
(3) - F.R. Arutyunyan and V.A. Tumanyan, Soviet Phys-Uspekhi 83, 339 (1964); R.H. Milburn, Phys. Rev. Letters 10, 75 (1963).
(4) - J.H. Hubbel, J. Appl. Phys. 30, 981 (1959).
(5) - H. Arenhövel, Proc. Intern. Conf. on Photonuclear Reactions and Applications, Asilomar (1973).
(6) - E. Hayward, Photonuclear Reactions, NBS Monograph 118 (1970).
(7) - H. Arenhövel and W. Greiner, Prog. in Nucl. Phys. 10, 167 (1968).
(8) - H.E. Jackson and K.J. Wetzel, Phys. Rev. Letters 22, 1008 (1969).
(9) - R. Moreh, D. Salzmann and G. Bon-David, Phys. Letters 34B, 494 (1971).
(10) - F. Ehlotzky and G.C. Sheppey, Nuovo Cimento 33, 1185 (1964).
(11) - G. Jarlskog and al., Measurement of Delbrück Scattering and Observation of Photon Splitting at High Energies, DESY 73/4 (1973).
(12) - H. Cheng and T.T. Wu, Phys. Rev. 182, 1873 (1969); Phys. Rev. 182, 1899 (1969); Phys. Rev. Letters 22, 666 (1969); DESY 71/69 (1971); V. Costantini, B. De Tollis and G. Pistoni, Nuovo Cimento 2A, 733 (1971).
(13) - J. Moffatt and M.W. Stringfellow, Proc. Roy. Soc. A 254, 242 (1960).
(14) - E.G. Fuller and E. Hayward, Phys. Rev. 101, 692 (1956).
(15) - E.G. Fuller and E. Hayward, Nuclear Phys. 30, 613 (1962).
(16) - J. Eisenberg and W. Greiner, Nuclear Excitation Mechanisms (North-Holland, Amsterdam, 1969).
(17) - H. Arenhövel and E. Hayward, Phys. Rev. 165, 1170 (1968).
(18) - E. Hayward, W.C. Barber and J. Sazoma, Phys. Rev., to be published.
(19) - G. Jacob and T.A.H. Maris, Rev. Mod. Phys. 45, 6 (1973).
(20) - B.M. Spicer, Adv. Nuclear Phys. (Plenum pub. New York, 1969) vol. II .
(21) - F. Firk, Ann. Rev. Nucl. Science 20, (1970).
(22) - B.L. Berman, Atlas of Photoneutron cross sections obtained with monoenergetic photons, UCRL-74622.
(23) - A.C. Odian et al., Phys. Rev. 102, 837 (1956); 119, 348 (1961); M.G. Barton and J.H. Smith, Phys. Rev. 110, 1143 (1958); A.N. Gorbunov et al., Soviet Phys.-JETP 15, 520 (1962); 16, 27 (1963); I.R. van Hise et al., Phys. Rev. 139, 554 (1965); J. Garvey et al., Nuclear Phys. 70, 241 (1965); B 1, 483 (1967); G.G. Taran, Sov. J. Nuclear Phys. 7, 301 (1968).
(24) - S. Costa et al., Lett. Nuovo Cimento 2, 665 (1971); N.N. Kaushal et al., Phys. Rev. 175, 1330 (1968).
(25) - E.G. Fuller et al., Photonuclear Reaction Data NBS Special Publication 380 (1973).
(26) - C. Whitehead et al., Phys. Rev. 110, 941 (1958).
(27) - S. Penner and J. Leiss, Phys. Rev. 114, 1101 (1959).
(28) - S.N. Gardiner, J.L. Matthews and R.O. Owens, Proc. Intern. Conf. Asilomar (1973), Vol. I; J.L. Mathews, R.O. Owens, S.N. Gardiner and D. Findlay, Proc. Intern. Conf. Asilomar (1973), Vol. I.
(29) - G. Manuzio et al., Nuclear Phys. A 133, 22 (1969); M. Sanzone et al., Nuclear Phys. A 153, 401 (1970); S. Costa et al., Lett. Nuovo Cimento 1, 448 (1971); E. Mancini et al., Nuovo Cimento, in press.
(30) - G.M. Shklyarevskij, Soviet Phys-JETP 9, 1057 (1959); S. Fujii, Progr. Theor. Phys. 29, 374 (1963).
(31) - J.S. Levinger, Phys. Rev. 84, 43 (1955).
(32) - K.G. Dedrick, Phys. Rev. 100, 43 (1955); K. Gottfried, Nuclear Phys. 5, 557 (1958); A. Reitan, Nuclear Phys. 36, 56 (1962); T.A. Gabriel and R.G. Alsmiller, Phys. Rev. 182, 1035 (1969); E. Bramanis, Nuclear Phys. A 193, 323 (1972).
(33) - G.M. Shklyarevskij, Soviet Phys-JETP 14, 170 (1962); W. Weise, M.G. Huber and M. Danos, Z. Phys. 236, 176 (1970); W. Weise, Lett. Nuovo Cimento 4, 541 (1970); W. Weise and M.G. Huber, Nuclear Phys. A 162, 330 (1971); Proc. Intern. Conf. Asilomar (1973), Vol. I; W. Weise, Phys. Letters 38 B, 301 (1972), and preprint, to be published.

(34) - M. Fink, H. Hebsch and H. Kummerl, Nuclear Phys. A 186, 353 (1972).
(35) - W. Weise, Private Comunication.
(36) - A. Arima, G.E. Brown, H. Hyuga and M. Ichimura, Nuclear Phys. A 205, 27 (1973).
(37) - G.R. Satchler, Proc. Phys. Soc. 68 A, 1041 (1955).
(38) - R. Raphael and H. Uberall, Nuclear Phys. 85, 327 (1966).
(39) - H.G. Miller et al., Nuclear Phys. A 163, 637 (1971).
(40) - B.C. Cook et al., Phys. Rev. 143, 724 (1966); J.A. Rawlins et al., Nuclear Phys. A 122, 128 (1968); P.C. Nagle et al., Nuclear Phys. A 127, 669 (1969); Y.M. Arkatov et al., Sov. J. Nucl. Phys. 9, 271 (1969); K. Kayser et al., Z. Phys. 239, 447 (1970).
(41) - J.J. De Swart and R.E. Marshak, Physics 25, 1001 (1959).
(42) - F. Partovi, Annals of Physics 27, 79 (1964).
(43) - F.F. Liu, Phys. Rev. 138, B 1443 (1965); G. Barbiellini et al., Phys. Rev. 154, 988 (1967).
(44) - H.G. Muller and H. Arenhövel, Phys. Rev. C7, 1003 (1973).
(45) - J.M. Wychoff, Phys. Rev. 159, 953 (1967).
(46) - J.M. Poutisson and W. Dal Bianes, Nuclear Phys. A 199, (1973).
(47) - H.J. V. Eyb, H. Schier and B. Schoch, Intern. Conf. on Photonuclear Reactions and Applications, Asilomar (1973), 8C8-1.